ＡＶＦサイクロトロン
更新計画加速器

平成１４年４月５日
研究会「中間エネルギー軽イオンビームによる物理」
於いて、ＲＣＮＰ

大阪大学核物理研究センター　佐藤健次

Ｉ　更新の動機と期待される性能

○　いま、何故、更新計画か？
○　誰も気付かなかったサイクロの忘れ物に気付いた
○　エネルギーのずれの二乗による非線形縦方向運動
①　シンクロトロン振動をさせる場合：大強度モード
②　フラットトップ加速でシンクロトロン振動をさせない場合：高分解能モード

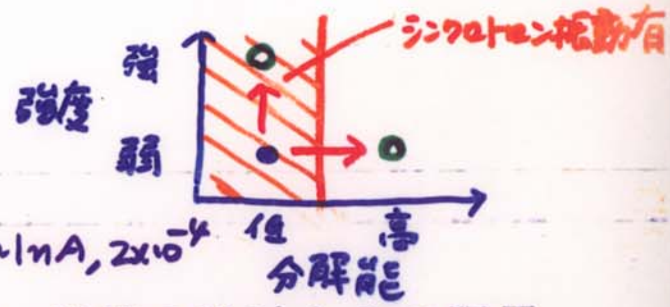

II　従来の成果を反映させた要素・設備の設計とその限界

○　要素と設備の重要性
（鉄芯温度の安定化とフラットトップ加速）
○　可変粒子と可変エネルギーの実現による限界
○　短時間で所定の運転条件を実現する技術の開発

III　検討中のサイクロトロンの機種とその前段加速器

○　主加速器リングサイクロの入射器に徹した設計、または、さらに単独の性能を高めた設計
1　小型常伝導リングサイクロトロン
2　小型超伝導リングサイクロトロン
3　ハイブリッド・サイクロトロン（常伝導、超伝導）
4　ＡＶＦサイクロトロン（常伝導、超伝導）

付録　ＦＦＦＦＡＧ(シンクロ)サイクロトロンから
FMＦＦＡＧシンクロサイクロトロンへ
○　パルスビームの生成と後段シンクロトロンへの道

Fixed-Field Alternating-Gradient Particle Accelerators*

FFAG

K. R. Symon,† D. W. Kerst,‡ L. W. Jones,§ L. J. Laslett,‖ and K. M. Terwilliger§
Midwestern Universities Research Association

(Received June 6, 1956)

MURA

It is possible, by using alternating-gradient focusing, to design circular accelerators with magnetic guide fields which are constant in time, and which can accommodate stable orbits at all energies from injection to output energy. Such accelerators are in some respects simpler to construct and operate, and moreover, they show promise of greater output currents than conventional synchrotrons and synchrocyclotrons. Two important types of magnetic field patterns are described, the radial-sector and spiral-sector patterns, the former being easier to understand and simpler to construct, the latter resulting in a much smaller accelerator for a given energy. A theory of orbits in fixed-field alternating-gradient accelerators has been worked out in linear approximation, which yields approximate general relationships between machine parameters, as well as more accurate formulas which can be used for design purposes. There are promising applications of these principles to the design of fixed-field synchrotrons, betatrons, and high-energy cyclotrons.

INTRODUCTION

Alternating-gradient (AG) focusing[1] provides a high degree of stability for both radial and vertical modes of betatron oscillations in circular particle accelerators. This stability makes possible the construction of many kinds of circular accelerators with magnetic guide fields which are constant in time, called fixed-field alternating-gradient (hereafter FFAG) accelerators. These machines contain stable equilibrium orbits for all particles from the injection energy to the output energy. These orbits may all be in an annular ring, as in a synchrotron or betatron; the magnetic field must then change rapidly with radius to provide orbits for the different energy particles. If the guide field gradient is made independent of azimuth, one of the modes of betatron oscillation is clearly unstable. Application of alternating-gradient focusing, however, can keep both modes of betatron oscillation stable even with the rapid radial change of magnetic field. Circular particle accelerators can be classified into four groups according to the type of guide field they use: fixed-field constant-gradient (conventional cyclotrons, synchrocyclotrons, and microtrons), pulsed-field constant-gradient (weak-focusing synchrotrons and betatrons), pulsed-field alternating-gradient (AG synchrotrons), and fixed-field alternating-gradient (FFAG synchrotrons, betatrons, and cyclotrons).

Two types of FFAG design appear the most practical. The radial-sector type[2] achieves AG focusing by having the fields in the successive focusing and defocusing magnets vary in the same way with radius but with alternating signs (or in certain cases alternating magnitudes). Since the orbit in the reverse field magnet bends away from the center, the machine is considerably larger than a conventional AG machine[1] of the same energy having an equal-peak magnetic field. This serious disadvantage is largely overcome in the spiral-sector type[3] in which the magnetic field consists of a radially increasing azimuthally independent field on which is superimposed a radially increasing azimuthally periodic field. The ridges (maxima) and troughs (minima) of the periodic field spiral outward at a small angle to the orbit. The radial separation between ridges is small compared to the radial aperture. The particle, crossing the field ridges at a small angle, experiences alternating-gradient focusing. Since the fields need not be reversed anywhere, the circumference of this machine can be comparable to that of an equivalent conventional AG machine.

FFAG synchrotrons have a number of important advantages over conventional synchrotrons. A major one is beam intensity. Since the magnetic field is time-independent in an FFAG synchrotron, the beam pulse rate is determined only by the repetition rate of the radio-frequency modulation cycle. In a conventional synchrotron, the beam pulse rate is limited by the time to complete the pulsed magnetic field cycle. It is reasonable to assume that frequency-modulation repetition rates can be made considerably higher than field recycling rates. Another reason for high beam intensity is the large injection aperture possible in the FFAG designs (larger for the radial sector than for the spiral sector). Other advantages of the FFAG synchrotron are engineering and maintenance simplifications. The direct-current magnet power supply is simpler and cheaper to construct and to maintain than a pulsed supply. The magnets do not have to be laminated, there are no eddy current problems, and remanent field and saturation difficulties are less serious than in pulsed-field

* Supported by National Science Foundation.

† University of Wisconsin, Madison, Wisconsin.
‡ University of Illinois, Champaign, Illinois.
§ University of Michigan and Michigan Memorial Phoenix Project, Ann Arbor, Michigan.
‖ Iowa State College Institute for Atomic Research, Ames, Iowa.

[1] Courant, Livingston, and Snyder, Phys. Rev. 88, 1190 (1952).

[2] K. R. Symon, Phys. Rev. 98, 1152(A) (1955). This structure was also suggested independently earlier by T. Ohkawa, University of Tokyo, Tokyo, Japan at a Symposium on Nuclear Physics of the Physical Society of Japan in October, 1953 (private communication), and independently by H. Snyder at Brookhaven National Laboratory.

[3] Suggested by D. W. Kerst [Kerst, Terwilliger, Jones, and Symon, Phys. Rev. 98, 1153(A) (1955)].

Courant, Snyder, Livingood ⇒ AG集束(強集束)

Q-mag.

Reprinted from *Phys. Rev.* ***103***, *1837–1859 (1956)*;

injection) is given as follows (see Fig. 22):

$$D=\frac{1}{2\pi}\cos^{-1}\left[\frac{\Delta\phi}{\phi_0}-1\right]. \tag{14.1}$$

In order to miss an injector structure, a certain minimum rate of acceleration (rate of rise of flux) at injection is required; this will reduce the duty factor in practice.

Since the particle equilibrium orbit is not circular and since its radius changes with acceleration, the relationship between $\Delta\phi$ and the momentum increase differs from that for conventional betatrons.

The voltage gain per revolution is, in Gaussian units,

$$V=(1/c)(d\phi/dt), \tag{14.2}$$

where ϕ is the flux in the betatron core. The rate of increase in energy is therefore

$$\frac{dE}{dt}=\left(\frac{e\omega}{2\pi c}\right)\frac{d\phi}{dt}, \tag{14.3}$$

where $\omega/2\pi$ is the frequency of revolution [Eq. (10.3)]. We have, therefore,

$$Rdp=\frac{dE}{\omega}=\left(\frac{e}{2\pi c}\right)d\phi, \tag{14.4}$$

and the required accelerating flux change is determined by

$$\phi_2-\phi_1=\frac{2\pi c\bar{R}}{e}(p_2-p_1), \tag{14.5}$$

where

$$\bar{R}=\frac{1}{p_2-p_1}\int_{p_1}^{p_2}Rdp. \tag{14.6}$$

If k is constant, we have, by Eq. (5.14),

$$\bar{R}=R_2\left(\frac{k+1}{k+2}\right)\frac{1-(p_1/p_2)^{(k+2)/(k+1)}}{1-(p_1/p_2)}$$

$$\doteq\left(\frac{k+1}{k+2}\right)R_2, \quad \text{if} \quad p_1\ll p_2. \tag{14.7}$$

With FFAG guide fields in the 20- to 300-Mev energy range, the duty factor could be increased by more than a factor of 10^4 over that in existing betatrons and synchrotrons. The beam current increase would probably be less because of space-charge effects at injection.

In pulsed-field betatrons, large amounts of energy are stored in the pulsed-guide field magnet gap, and equipment capable of handling the large circulating currents and voltages must be used. In FFAG betatrons, only the accelerating core is pulsed, and it would be a closed iron circuit which would require much less energy storage, and therefore a much smaller condenser bank and less ac power equipment.

Either the radial-sector or the spiral-sector type of FFAG magnet could be used for electron betatron acceleration up to a few hundred Mev, and the design would be subject to the same considerations as discussed above for synchrotrons. Since the core flux change for a given particle momentum increase is proportional to the particle period of revolution, the smaller circumference of the spiral sector type is doubly important for betatrons. In focusing magnets designed for the betatron energy range, an N of 10 to 30 appears more suitable than the higher N values suggested for multi-Bev synchrotrons.

The output beam of electrons from an FFAG betatron would be nearly monoenergetic and spread over a long time corresponding to the duty factor. Present betatrons and synchrotrons achieve a lengthened output beam pulse at the expense of energy homogeneity, since the electrons are in a sinusoidally varying field at essentially constant radius. This and the prospect of beam currents approaching time-average values of milliamperes makes this an attractive accelerator for electrons from a few Mev to several hundred Mev.

15. FFAG Cyclotrons

To make semirelativistic particles revolve in a cyclotron at constant frequency and in orbits that are approximately circles, it is necessary to have the average magnetic field increase with radius. In order to avoid the resultant axial defocusing, alternating-gradient focusing may be employed. There are a number of possible magnetic field configurations for such a fixed-field alternating-gradient cyclotron. The first such cyclotron was proposed by Thomas.[5] The Thomas cyclotron is essentially a radial-sector FFAG machine having three or more sectors with a roughly sinusoidal field flutter. Thomas showed that such a machine has stable orbits for energies up to a limit depending upon the number of sectors. A considerable amount of experimental and theoretical work on the Thomas

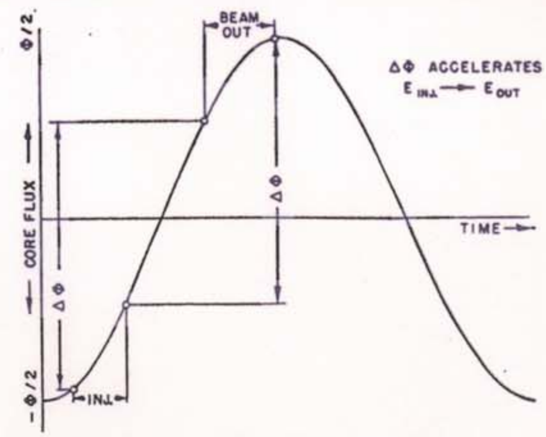

FIG. 22. Time dependence of betatron flux showing duty factor.

I　更新の動機と期待される性能

サイクロトロンにおける非線形ビーム軌道理論の必要性

—エネルギーのずれの二乗などの非線形項の効果—

ultra-precise beam（超高品質ビーム）が磁場の僅かなずれで、
エネルギー幅が大幅に悪くなる。

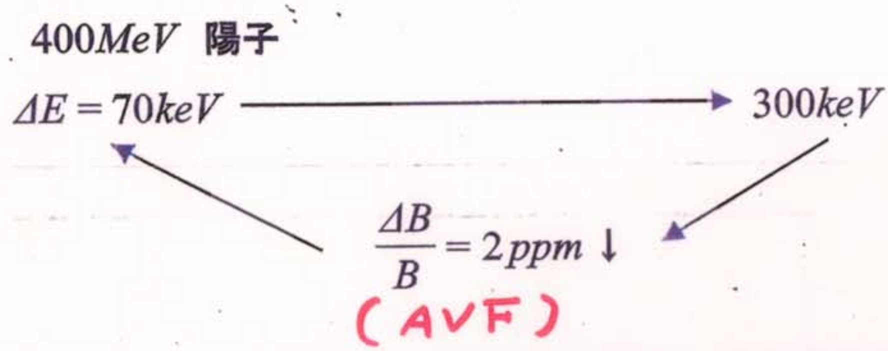

イオン源
↓
AVF
↓
リング
↓

この原因をエネルギーのずれの二乗などの非線形項の効果とすると、定量的に説明できる可能性が出て来た。

超高品質ビームの実践

電磁石の鉄芯温度をコイルの冷却水温度を制御して磁場を長時間安定にできた結果である。

極超高品質ビームへの挑戦

$\Delta E = 70 keV$　自身が非線形項の効果の結果とすると矯正できるはず！

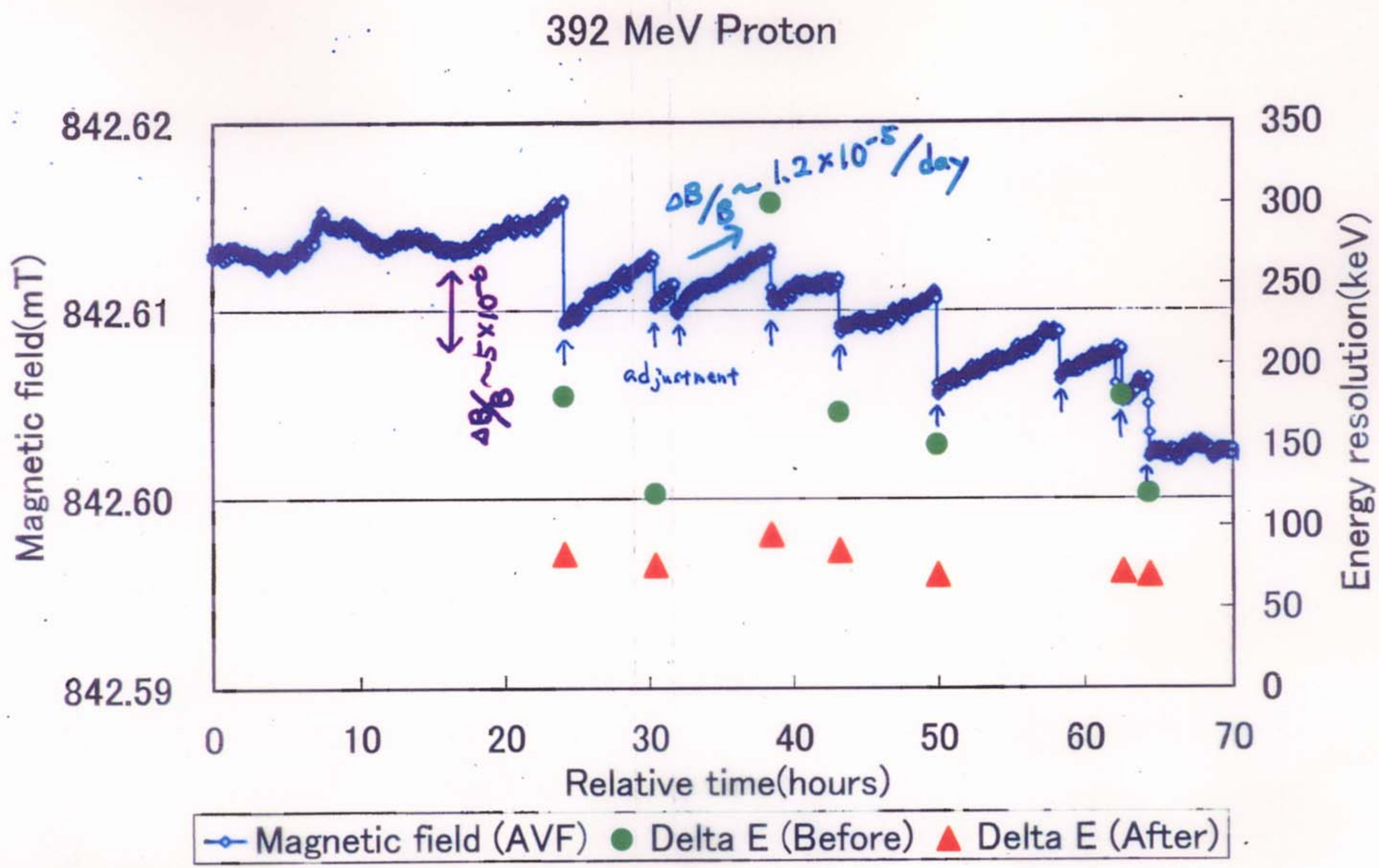
392 MeV Proton
842.62
842.61
842.60
842.59
Magnetic field(mT)
0
10
20
30
40
50
60
70
Relative time(hours)
350
300
250
200
150
100
50
0
Energy resolution(keV)
ΔB/B ~ 5×10^-6
ΔB/B ~ 1.2×10^-5 /day
adjustment
Magnetic field (AVF)
Delta E (Before)
Delta E (After)

Cylindrical coordinate: (r, θ, z)

Equations of motion in a median plane : $z = 0, \dot{z} = 0$

$$\begin{cases} \gamma = \dfrac{1}{\sqrt{1 - \left(\dfrac{\dot{r}}{c}\right)^2 - \left(\dfrac{r\dot{\theta}}{c}\right)^2}} \\ m_0 \gamma \ddot{r} + m_0 \dot{\gamma} \dot{r} - m_0 \gamma r \dot{\theta}^2 = q r \dot{\theta} B_z(r) \\ m_0 c^2 \dot{\gamma} = \dfrac{qV}{2\pi} \dot{\theta} \cos\phi \end{cases}$$

where $\phi = \omega_{rf} t + \phi_{rf} - h\theta$

$q > 0, B_z(r) < 0$ *so that* $\dot{\theta} > 0$

Equations of motion of a reference particle

$$\begin{cases} \gamma_n = \dfrac{1}{\sqrt{1 - \left(\dfrac{\dot{r}_n}{c}\right)^2 - \left(\dfrac{r_n \dot{\theta}_n}{c}\right)^2}} \\ m_0 \gamma_n \ddot{r}_n + m_0 \dot{\gamma}_n \dot{r}_n - m_0 \gamma_n r_n \dot{\theta}_n^{\,2} = q r_n \dot{\theta}_n B_{zn}(r_n) \\ m_0 c^2 \dot{\gamma}_n = \dfrac{q V_n}{2\pi} \dot{\theta}_n \cos\phi_n \end{cases}$$

$$\frac{\dot{\theta}-\dot{\theta}_n}{\dot{\theta}_n}=-\frac{r-r_n}{r_n}-\frac{\left(\frac{\dot{r}_n}{c}\right)^2}{\left(\frac{r_n\dot{\theta}_n}{c}\right)^2}\frac{\dot{r}-\dot{r}_n}{\dot{r}_n}+\frac{\frac{1}{\gamma_n^{\ 2}}}{\left(\frac{r_n\dot{\theta}_n}{c}\right)^2}\frac{\gamma-\gamma_n}{\gamma_n}$$

$$-\frac{\frac{1}{\gamma_n^{\ 2}}\left\{\frac{3}{2}-\frac{1}{\gamma_n^{\ 2}}-\frac{3}{2}\left(\frac{\dot{r}_n}{c}\right)^2\right\}}{\left(\frac{r_n\dot{\theta}_n}{c}\right)^2}\left(\frac{\gamma-\gamma_n}{\gamma_n}\right)^2$$

$$\frac{\dot{\theta}^2-\dot{\theta}_n^{\ 2}}{\dot{\theta}_n^{\ 2}}=-\,2\frac{r-r_n}{r_n}-2\frac{\left(\frac{\dot{r}_n}{c}\right)^2}{\left(\frac{r_n\dot{\theta}_n}{c}\right)^2}\frac{\dot{r}-\dot{r}_n}{\dot{r}_n}+2\frac{\frac{1}{\gamma_n^{\ 2}}}{\left(\frac{r_n\dot{\theta}_n}{c}\right)^2}\frac{\gamma-\gamma_n}{\gamma_n}$$

$$-3\frac{\frac{1}{\gamma_n^{\ 2}}}{\left(\frac{r_n\dot{\theta}_n}{c}\right)^2}\left(\frac{\gamma-\gamma_n}{\gamma_n}\right)^2$$

Equation of longitudinal motion(phase oscillation)
without synchro-betatron coupling

Definition of deviation

$$\phi-\phi_n=-h(\theta-\theta_n)+(\omega_{rf}-\omega_{rf,n})t+\phi_{rf}$$

$$\dot{\phi}-\dot{\phi}_n=-h(\dot{\theta}-\dot{\theta}_n)+\omega_{rf}-\omega_{rf,n}+\dot{\phi}_{rf}$$

$$x=r-r_n$$

$$\Gamma=\frac{\gamma-\gamma_n}{\dot{\theta}_n}$$

Definition of deviation

$$B_z(r)=B_{zn}(r_n)\left(1-n\frac{r-r_n}{r_n}\right)+b\ :n=-\frac{r_n}{B_{zn}(r_n)}\frac{dB_{zn}(r)}{dr}\bigg|_{r=r_n}$$

$$V=V_n+v$$

field index

Reference particle condition

$$qB_{zn}(r_n)=\frac{m_0\gamma_n\ddot{r}_n}{r_n\dot{\theta}_n}-\frac{m_0\dot{\gamma}_n\dot{r}_n}{r_n\dot{\theta}_n}-m_0\gamma_n\dot{\theta}_n$$

First-step approximation $:\dot{r}_n\approx 0,\ddot{r}_n\approx 0$

so that $r_n\approx\dfrac{1}{\sqrt{1-(\frac{r_n\dot{\theta}_n}{c})^2}}$

Further approximation $:\dot{\gamma}_n\approx 0$

Definition of transition-γ $:\gamma_t^{\,2}=1-n$

the leading term

Q ~ 0

Equations of longitudinal motion (phase oscillation) without synchro-betatron coupling

linear theoory

$$\begin{cases} \dot{\phi} - \dot{\phi}_n = P\Gamma^2 - Q\Gamma - R + U\dot{x} \\ \dot{\Gamma} = S(\cos\phi - \cos\phi_n) + S\dfrac{v}{V_n}\cos\phi_n \end{cases}$$

$$\ddot{x} + lx = m\Gamma + n\Gamma^2 + p$$

$$\begin{cases} \dot{\phi} = -R = 0 \\ \\ lx = m\Gamma + p \end{cases}$$

where

$$\begin{cases} P = -\left\{\dfrac{3}{2} - \dfrac{1}{\gamma_n^{\,2}} - \dfrac{2}{\gamma_t^{\,2}}\left(\dfrac{3}{4} - \dfrac{1}{\gamma_n^{\,2}}\right)\right\}\dfrac{hc^4}{\gamma_n^{\,4} r_n^{\,4}\dot{\theta}_n} \\ Q = \left(\dfrac{1}{\gamma_n^{\,2}} - \dfrac{1}{\gamma_t^{\,2}}\right)\dfrac{hc^2}{\gamma_n r_n^{\,2}} \\ R = -\left(\dfrac{hq}{m_0\gamma_t^{\,2}\gamma_n} b + \omega_{rf} - \omega_{rf,n} + \dot{\phi}_{rf}\right) \\ S = \dfrac{qV_n}{2\pi m_0 c^2} \\ U = -\dfrac{h}{\gamma_t^{\,2}\gamma_n\dot{\theta}_n} \end{cases}$$

$$\begin{cases} l = \gamma_t^{\,2}\dot{\theta}_n^{\,2} \\ m = \dfrac{c^2\dot{\theta}_n}{\gamma_n r_n} \\ n = -2\left(\dfrac{3}{4} - \dfrac{1}{\gamma_n^{\,2}}\right)\dfrac{c^4}{\gamma_n^{\,4} r_n^{\,3}} \\ p = \dfrac{qr_n\dot{\theta}_n}{m_0\gamma_n} b \end{cases}$$

Hamiltonian formalism of longitudinal motion

because of constant parameters

Necessary condition : $\dot{\phi}_n = 0$

synchronous(isochronous)

$$\begin{cases} \dot{\phi} = -P\Gamma^2 - Q\Gamma - R \\ \dot{\Gamma} = S(\cos\phi - \cos\phi_n) \end{cases}$$

Hamiltonian

$$H = \int \dot{\phi}\, d\Gamma - \int \dot{\Gamma}\, d\phi$$

$$H = -\frac{1}{3}P\Gamma^3 - \frac{1}{2}Q\Gamma^2 - R\Gamma - S(\sin\phi - \phi\cos\phi_n)$$

Definition of $g(\Gamma)$

$$g(\Gamma) \equiv \frac{1}{3}P\Gamma^3 + \frac{1}{2}Q\Gamma^2 + R\Gamma$$

$$g'(\Gamma) = \frac{dg}{d\Gamma} = P\Gamma^2 + Q\Gamma + R = -\dot{\phi}$$

Behavior of $g(\Gamma)$ in case of $P < 0$

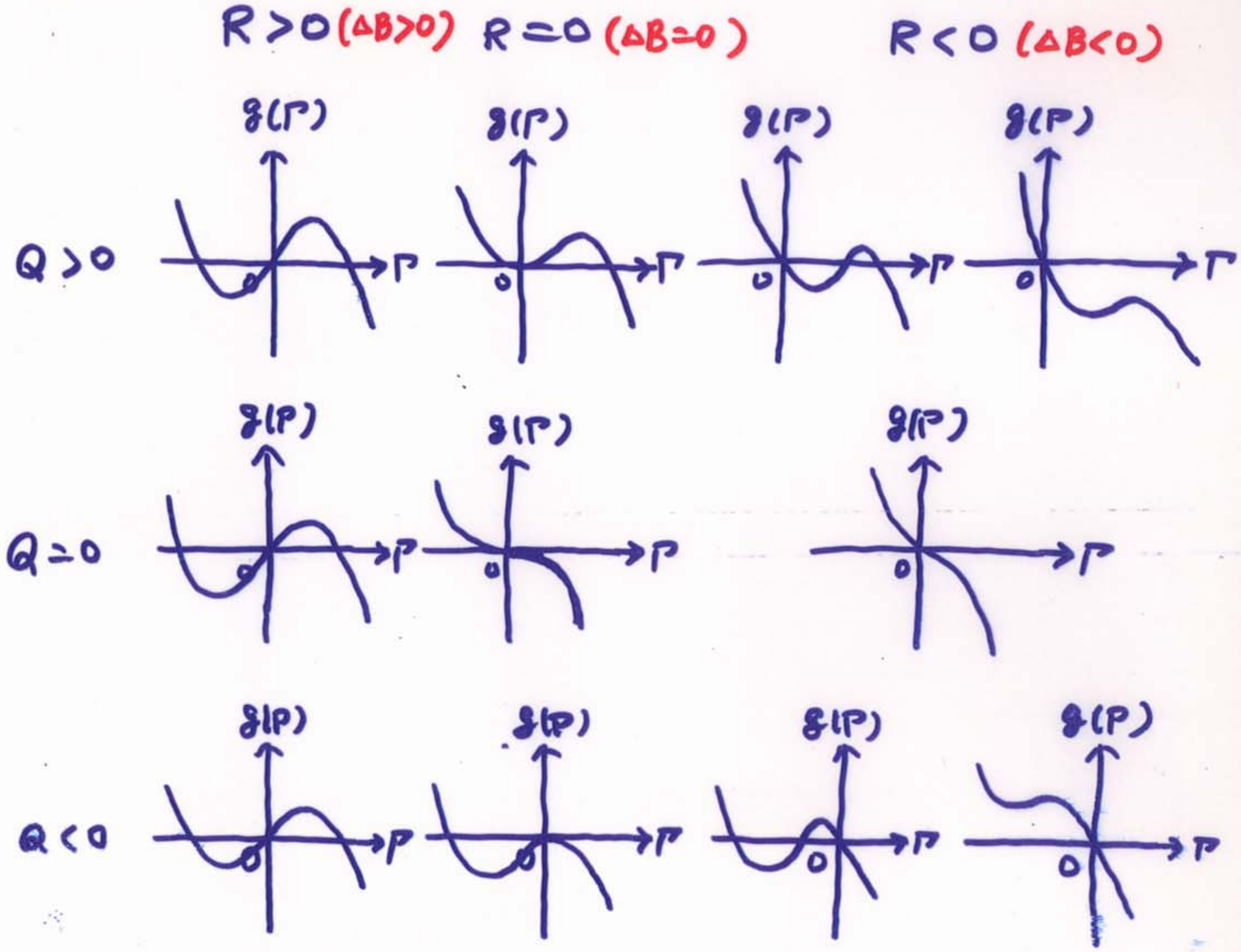

Where is cyclotron ?

Where is synchrotron ?

$$Q = \left(\frac{1}{\gamma_n^2} - \frac{1}{\gamma_t^2}\right)\frac{hc^2}{\gamma_n r_n^2}$$

$Q = 0$ case in cyclotrons

$R > 0$ ($\Delta B > 0$) $R = 0$ ($\Delta B = 0$) $R < 0$ ($\Delta B < 0$)

$Q=0$

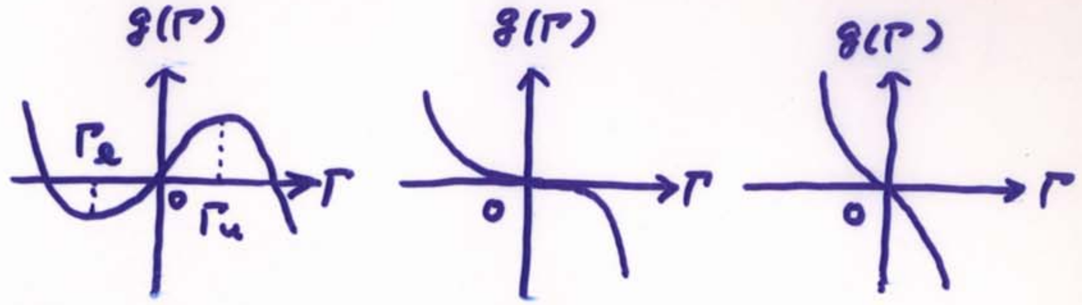

$$Q = 0 \implies \gamma_t^2 = \gamma_n^2$$

$$P = -\left\{\frac{3}{2} - \frac{1}{\gamma_n^2} - \frac{2}{\gamma_n^2}\left(\frac{3}{4} - \frac{1}{\gamma_n^2}\right)\right\}\frac{hc^4}{\gamma_n^4 r_n^4 \dot{\theta}_n}$$

$$R = -\left(\frac{h g}{m_0 \gamma_n^3} b + \omega_{rf} - \omega_{rf,n} + \dot{\phi}_{rf}\right)$$

Proper energy difference in case of $b < 0$

$$\frac{\Delta E}{E} = \frac{\dot{\theta}_n}{\gamma_n - 1}(\Gamma_u - \Gamma_e) \Leftarrow \dot{\phi} = 0,\ P\Gamma^2 + R = 0,\ \Gamma = \pm\sqrt{-\frac{R}{P}}$$

Numerical example : 50 MeV proton, $gV_n = 100$ keV, $h = 1$

$$\frac{\Delta E}{E} \simeq 4.18\sqrt{-\frac{b}{|B_{zn}|}} = 4.18\sqrt{\frac{\Delta B}{B}} \text{ when } \Delta B > 0$$

$-\frac{b}{\lvert B_{zn}\rvert}$	$\frac{\Delta E}{E}$	ΔE
1 ppm	4.18×10^{-3}	209 keV

1 ppm $= 1\times10^{-6} \Rightarrow \sqrt{1\times10^{-6}} = 10^{-3}$

Synchrotron oscillation in cyclotrons in case of local maximum and local minimum both for $g(\Gamma)$

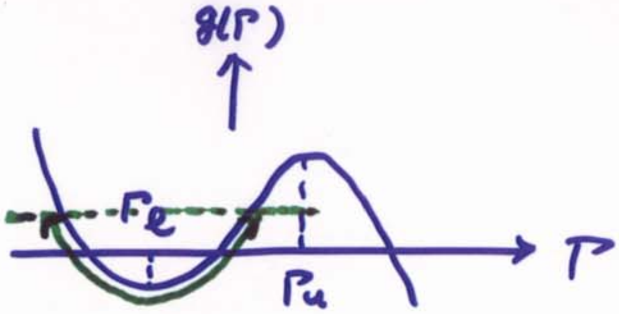

Synchrotron oscillation around Γ_e and/or Γ_u ?

Formalization

Definition

$$\begin{cases} \Gamma_e, \Gamma_u \longrightarrow \Gamma_0 \\ \phi_e, \phi_u \longrightarrow \phi_0 \end{cases}$$

Definition

$$\begin{cases} \underline{\eta} = \Gamma - \Gamma_0 \\ \underline{\Phi} = \phi - \phi_0 \end{cases}$$

Small amplitude approximation

$$\begin{cases}\dot{\Phi} = -P\eta^2 - (2P\Gamma_0 + Q)\eta \\ \dot{\eta} = S(\cos\phi_0 \cos\Phi - \sin\phi_0 \sin\Phi - \cos\phi_0)\end{cases}$$

$$|\eta| << 1, \quad \cos\Phi \approx 1, \quad \sin\Phi \approx \Phi$$

$$\begin{cases}\dot{\Phi} \approx -(2P\Gamma_0 + Q)\eta \\ \dot{\eta} \approx -\Phi S \sin\phi_0\end{cases}$$

$$\begin{cases}\ddot{\Phi} - \Phi(2P\Gamma_0 + Q)S\sin\phi_0 = 0 \\ \ddot{\eta} - \eta(2P\Gamma_0 + Q)S\sin\phi_0 = 0\end{cases}$$

$-(2P\Gamma_0 + Q)S\sin\phi_0 > 0$のとき単振動
シンクロトロン振動している。

シンクロトロン角速度　ω_{syn}　$:\omega_{syn} = \sqrt{-(2P\Gamma_0 + Q)S\sin\phi_0}$

METHODS OF RADIO FREQUENCY ACCELERATION IN FIXED FIELD ACCELERATORS WITH APPLICATIONS TO HIGH CURRENT AND INTERSECTING BEAM ACCELERATORS

K. R. SYMON AND A. M. SESSLER

Midwestern Universities Research Association (U.S.A.) *

(presented by K. R. Symon)

I. A Survey of ideas for radio frequency acceleration

A fixed field accelerator can accommodate at one time particles circulating at all energies between the injector and output energies. There thus becomes available a whole new class of accelerating mechanisms which appear to promise high intensity beams. Such high intensity, besides being of interest in a single accelerator, is of course essential for the operation of a double accelerator with interacting beams. These accelerating mechanisms are now being studied by analytic means as well as by the digital computer. In general, one is concerned with the energy gain of particles whose frequencies are a function of energy, as these particles are subject to various radio frequency accelerating gaps, whose voltages and frequencies may be secularly changed. Of the many possible arrangements, not all of which have been studied, the following seems to have particular promise. More calculations will have to be done before one can choose which of the following mechanisms or what combination of them is most efficient.

(a) *Conventional synchrotron acceleration at high repetition rate*

The most straightforward accelerating system is one which uses one or several synchronized accelerating gaps supplying a radio frequency voltage whose frequency is modulated as in conventional synchrotrons so as to accelerate a pulse of particles from the injection to the output energy. The only advantage of an FFAG magnet in this case is that the pulse repetition rate is now limited only

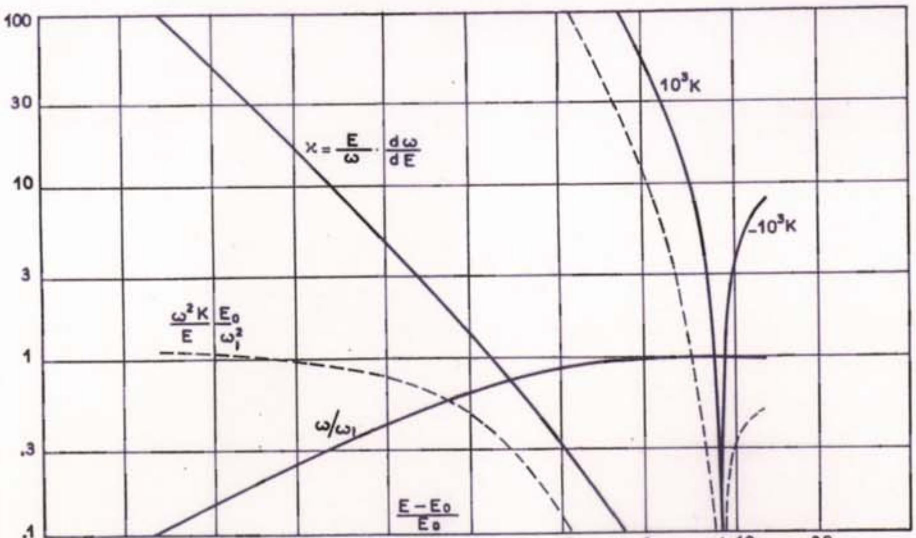

Fig. 1. Frequency versus energy $k = 82.5$

* Assisted by the National Science Foundation and the Office of Naval Research.

Reprinted from *Proc. of the CERN Symposium, 44–58 (1956)*; © CERN.

2/13

$\varphi_s = 0$

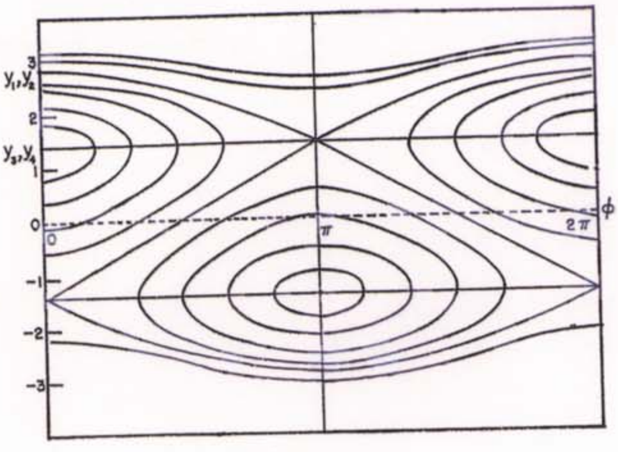

Fig. 6. Phase plane near transition $\eta = \eta_0$

$$W^* = \frac{E^*}{\omega_t}\left(1 + \frac{1}{3k}\frac{E^{*2}}{E_t^2}\right), \tag{54}$$

$$E^* = \omega_t W^* - \frac{1}{3k}\frac{\omega_t^3 W^{*3}}{E_t^2}; \tag{55}$$

We introduce the dimensionless variables

$$y = \left(\frac{4\pi}{k}\right)^{1/3}\left(\frac{hE_t}{V}\right)^{1/3}\frac{\omega_t W^*}{E_t}, \tag{56}$$

$$\varphi = h\,\Theta^* \tag{57}$$

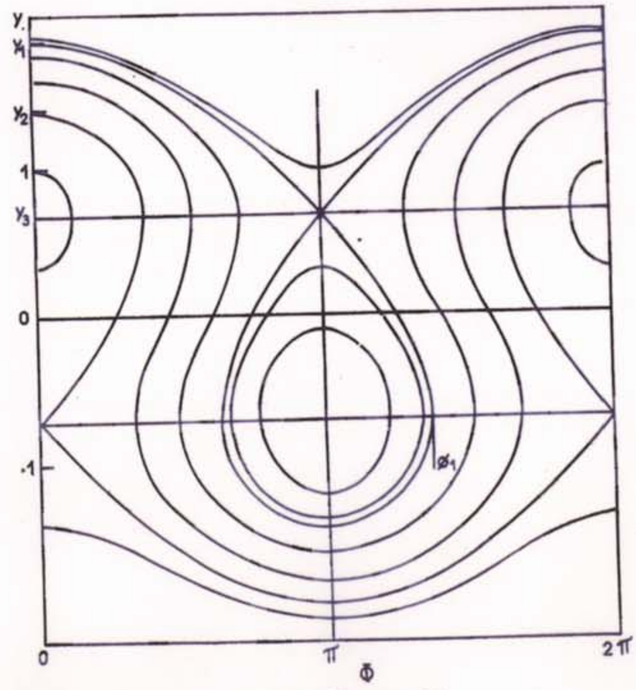

Fig. 7. Phase plane near transition $\eta = 25$

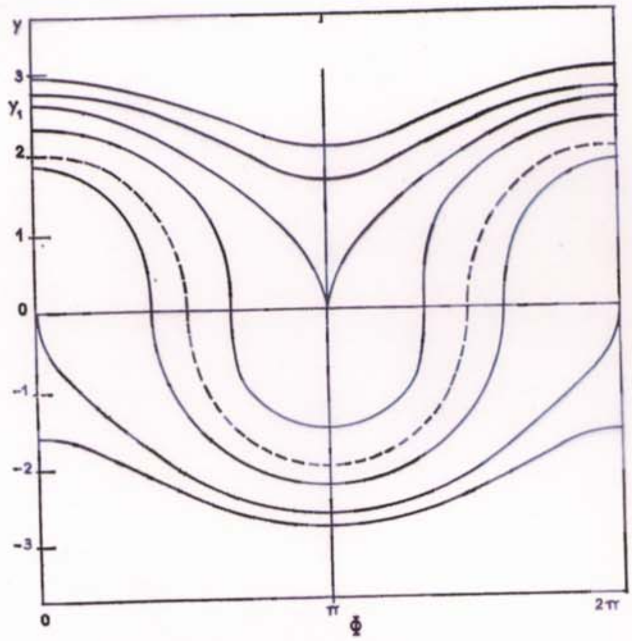

Fig. 8. Phase plane at transition $\eta = 0$

and the parameters

$$\eta = (2\pi^2 k)^{1/3}\,(hE_t/V)^{2/3}\,(1 - \nu/h\omega_t), \tag{58}$$

$$C = h\,H^*/V. \tag{59}$$

we may then write the Hamiltonian (29) in the form

$$-1/6\,y^3 + \eta\,y + \cos\varphi = C, \tag{60}$$

where we have again omitted terms independent of φ, y.

Graphs of eq. (60) for several values of C and η are shown in fig. 5, 6, 7, 8 and 9. We are particularly inter-

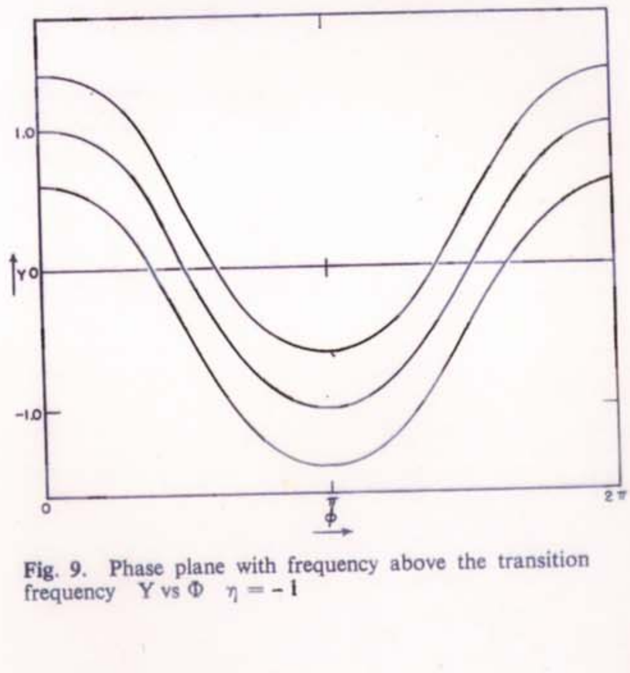

Fig. 9. Phase plane with frequency above the transition frequency Y vs Φ $\eta = -1$

Hamiltpnian formalism

$$\begin{cases} \dot{\Phi} = -P\eta^2 - (2P\Gamma_0 + Q)\eta \\ \dot{\eta} = S(\cos\phi_0 \cos\Phi - \sin\phi_0 \sin\Phi - \cos\phi_0) \end{cases}$$

変数変換

$P<0$ 　のとき

$$\xi \equiv \sqrt{-P}\left(\eta + \frac{2P\Gamma_0 + Q}{2P}\right)$$

$$\begin{cases} \dot{\Phi} = \xi^2 - \dfrac{(2P\Gamma_0 + Q)^2}{4P} \\ \dot{\xi} = \sqrt{-P}S(\cos\phi_0 \cos\Phi - \sin\phi_0 \sin\Phi - \cos\phi_0) \end{cases}$$

Hamiltonian

$$H = \int \dot{\Phi}\, d\xi - \int \dot{\xi}\, d\Phi$$

$$= \frac{1}{3}\xi^3 + \frac{(2P\Gamma_0 + Q)^2}{4P}\xi - \sqrt{-P}S(\cos\phi_0 \sin\Phi + \sin\phi_0 \cos\Phi - \Phi\cos\phi_0)$$

$$\xi^3 + \frac{3(2P\Gamma_0 + Q)^2}{4P}\xi = 3\left\{\sqrt{-P}S(\cos\phi_0 \sin\Phi + \sin\phi_0 \cos\Phi - \Phi\cos\phi_0) + H\right\}$$

see Symon and Sessler

Potential formalism of nonlinear oscillation

$$\xi\left(\xi^2+\frac{3(2P\Gamma_0+Q)^2}{4P}\right)=3\left\{\sqrt{-P}S(\cos\phi_0\sin\Phi+\sin\phi_0\cos\Phi-\Phi\cos\phi_0)+H\right\}$$

二乗

$$\xi^2\left(\xi^2+\frac{3(2P\Gamma_0+Q)^2}{4P}\right)^2=9\left\{\sqrt{-P}S(\cos\phi_0\sin\Phi+\sin\phi_0\cos\Phi-\Phi\cos\phi_0)+H\right\}^2$$

$\xi^2=\dot{\Phi}-\dfrac{(2P\Gamma_0+Q)^2}{4P}$ を代入

$$\dot{\Phi}^3+\frac{3(2P\Gamma_0+Q)^2}{4P}\dot{\Phi}^2-4\left\{\frac{(2P\Gamma_0+Q)^2}{4P}\right\}^3$$
$$=9\left\{\sqrt{-P}S(\cos\phi_0\sin\Phi+\sin\phi_0\cos\Phi-\Phi\cos\phi_0)+H\right\}^2$$

この三次方程式を解けば、$\dot{\Phi}$ が Φ の関数として求まる。

その解より、運動エネルギーと位置エネルギーの形に書ける。

$$E=\frac{1}{2}\dot{\Phi}^2+U(\Phi)=一定$$

↑

potential

$\dfrac{d\dot{\Phi}}{d\Phi}=0$ より *unstable fixed points* が求まる

以下省略

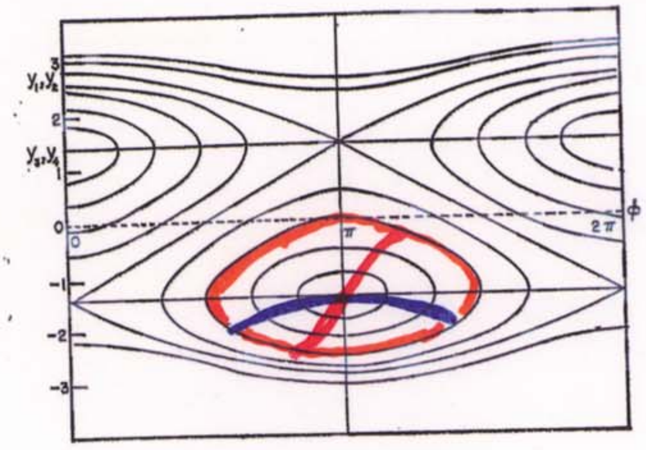

Fig. 6. Phase plane near transition $\eta = \eta_c$

$$W^* = \frac{E^*}{\omega_t}\left(1 + \frac{1}{3k}\frac{E^{*2}}{E_t^2}\right), \tag{54}$$

$$E^* = \omega_t W^* - \frac{1}{3k}\frac{\omega_t^3 W^{*3}}{E_t^2}. \tag{55}$$

We introduce the dimensionless variables

$$y = \left(\frac{4\pi}{k}\right)^{1/3}\left(\frac{hE_t}{V}\right)^{1/3}\frac{\omega_t W^*}{E_t}, \tag{56}$$

$$\varphi = h\,\Theta^* \tag{57}$$

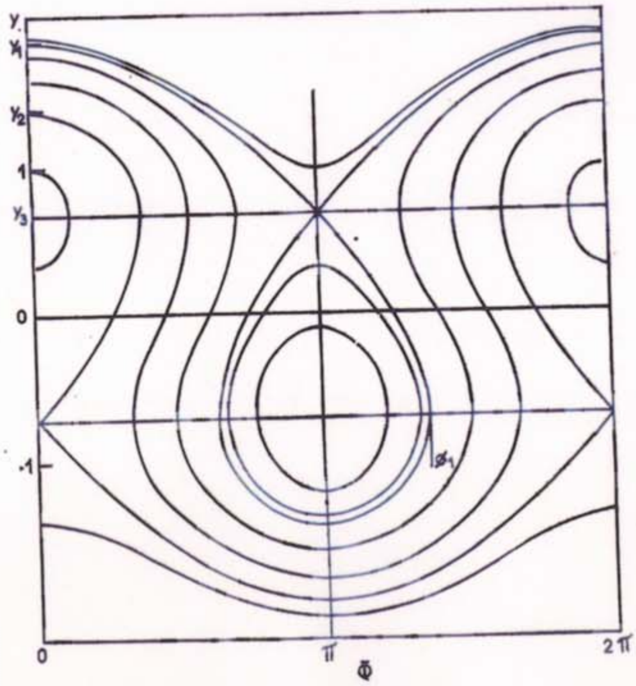

Fig. 7. Phase plane near transition $\eta = 25$

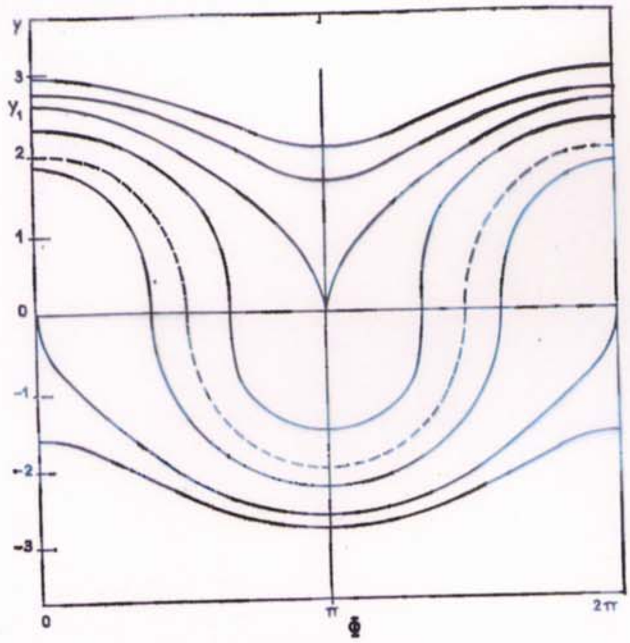

Fig. 8. Phase plane at transition $\eta = 0$

and the parameters

$$\eta = (2\pi^2 k)^{1/3}\,(hE_t/V)^{2/3}\,(1 - \nu/h\omega_t), \tag{58}$$

$$C = h\,H^*/V. \tag{59}$$

we may then write the Hamiltonian (29) in the form

$$-1/6\,y^3 + \eta y + \cos\varphi = C, \tag{60}$$

where we have again omitted terms independent of φ, y.

Graphs of eq. (60) for several values of C and η are shown in fig. 5, 6, 7, 8 and 9. We are particularly inter-

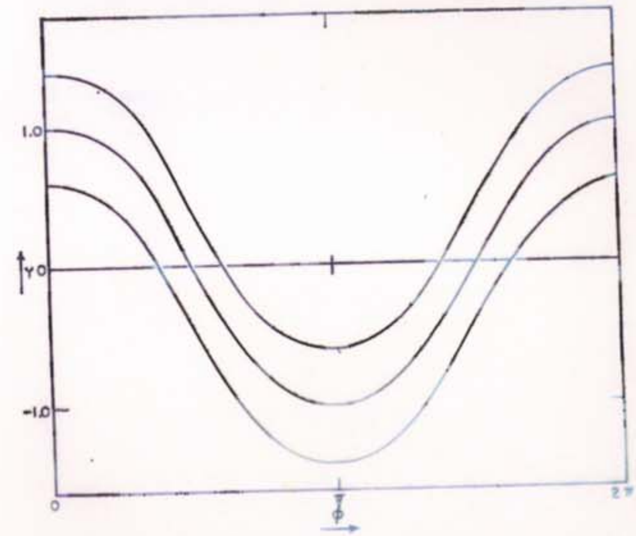

Fig. 9. Phase plane with frequency above the transition frequency Y vs Φ $\eta = -1$

Specification of cyclotrons

	Injector	Ring cyclotron
No. of sector magnets	3	6
Injection radius(cm)		200
Extraction radius(cm)	100	400
Magnet gap(cm)	20.7(min)	6.0
Max. field(kG)	19.5	17.5
No. of trim coils	16	36
No. of acceleration cavity	1	3
Frequency(MHz)	5.5 - 19	30 - 52
Max. voltage(kV)	70	550
No. of flat-topping cavity		1
FT frequency(MHz)		90 - 156
FT Max. voltage(kV)		170
Ion sources(external)	HIPIS ECR	

Suppression of synchrotron oscillation by flat-topping

Flat–topping of Ring Cyclotron

High–quality beam due to: a wide phase acceptance
a single–turn extraction

$m = 3$

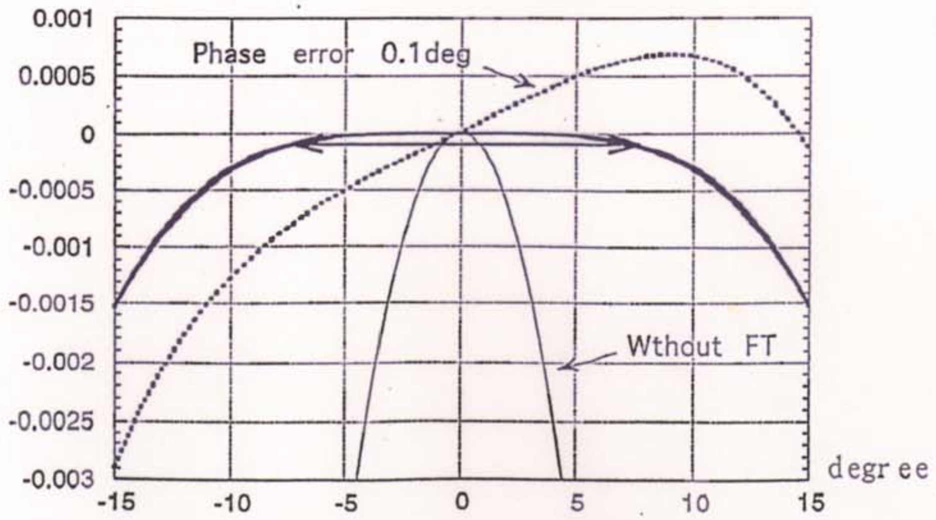

Effective acceleration voltage vs phase

$$V_{rf} = V_0 \left\{ \cos(\omega_{rf} t) - \frac{1}{m^2} \cos(m \omega_{rf} t) \right\}$$

Equations of longitudinal motion in case of flat-topping rf acceleration voltage

$$\begin{cases} \dot{\phi} - \dot{\phi}_n = -P\Gamma^2 - Q\Gamma - R + \cancel{U\ddot{x}} \\ \dot{\Gamma} = 0 \end{cases}$$

$$\cancel{\ddot{x}} + lx = m\Gamma + n\Gamma^2 + p$$

$\Gamma = \text{const.} \Longrightarrow$ **no synchrotron oscillation!**

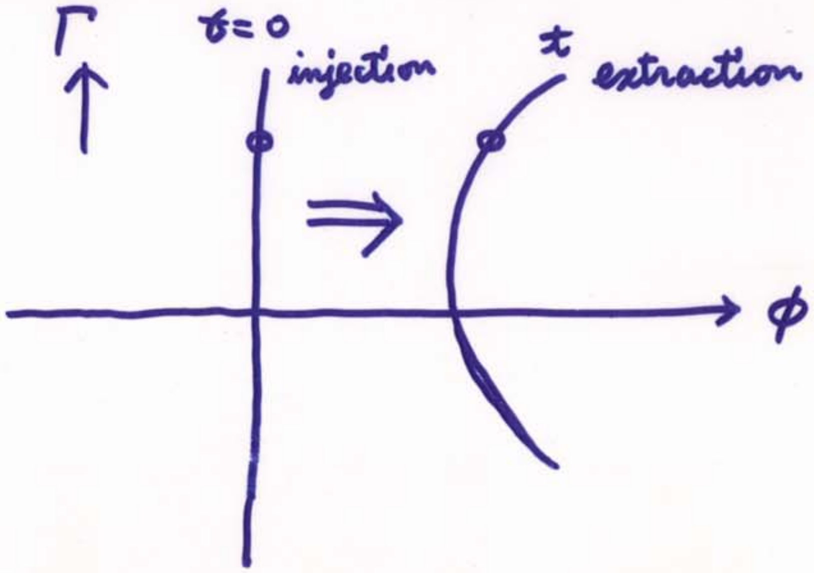

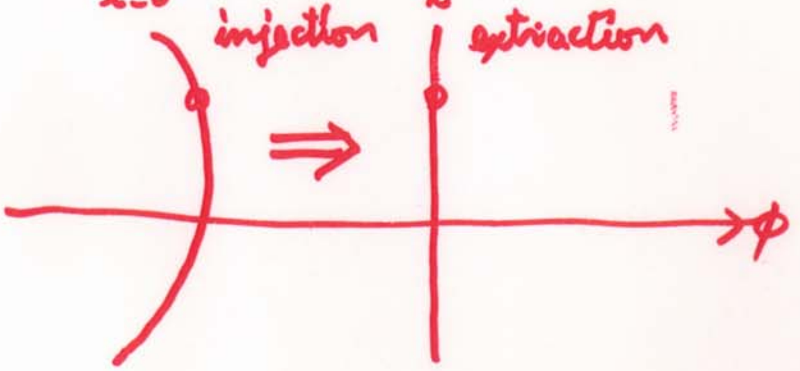

入射ビームの整形が必要!
ビーム輸送で言えば
六極電磁石のような
もの

FF FFAG

固定磁場(FF), 固定周波数(FF)のシンクロ・サイクロトロン

今後検討して行きたい課題

$$Q=\left(\frac{1}{\gamma_{t}^{2}}-\frac{1}{\gamma_{x}^{2}}\right)\frac{hc^{2}}{\gamma_{n}\gamma_{n}^{2}}$$

1. 世界のサイクロで $\frac{\Delta E}{E}\sim 1\times10^{-3}$ の理由

$\dot{\phi}_{e}=0$ または $\dot{\phi}_{u}=0$ $\Longrightarrow$ シンクロトロン振動を発生させる

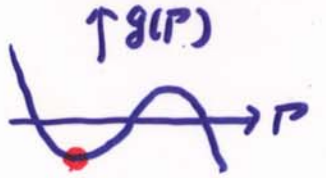

① $Q\neq0$ しかし $R=0$: $\Gamma_{u}-\Gamma_{e}=-\frac{Q}{P}$

② $R\neq0$ しかし $Q=0$: $\Gamma_{u}-\Gamma_{e}=2\sqrt{-\frac{R}{P}}\ \begin{pmatrix}P<0\\R>0\end{pmatrix}$

2. $\ell x=m\Gamma+m\Gamma^{2}+p$ と言う非線形性とマルチターン取り出しとの関係

同一の取り出し半径を、異なるエネルギーの粒子が通過できるのではないか？

3. 2つの運転モードの可能性

① 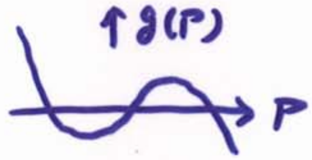

大強度ビーム・モード
シンクロトロン振動による集束力

② 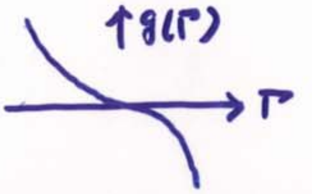

高品質ビーム・モード
シンクロトロン振動しない

4. 非線形高周波補償装置

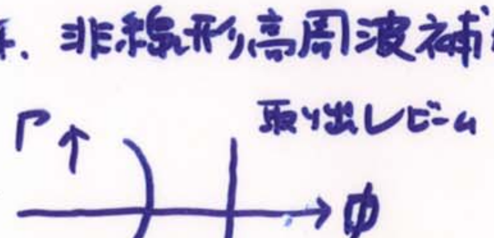

入射ビームを) と整形する装置

5. シンクロトロン振動高周波整合装置：線形加速器でも可！

Lists of Cyclotrons

識別番号	研究所の名称		k値	ΔE/E
C1	Louvain-Ia-Neuve(BELGIUM)	85MeV, p,,,h.I.	K=110	0.003
C4	Winnipeg(U.of Man)(CANADA)	50MeV, p,....		0.012
C5	Vancouver(TRIUMF)(CANADA)	520MeV, H-		0.002
C6	Santiago(U.de Chile)(CHILE)	10MeV, p,...		0.01
C10	Shanghai(INR)(CHINA)	30MeV, p,...		0.01
C23	Berlin(HMI)(GERMANY)	72MeV, p,.,h.I.	k=130	0.001
C25	Julich(KFK)(GERMANY)	45MeV, H-,..,	k=180	0.003
C27	Karlsruhe(KFK)(GERMANY)	42MeV, H-		0.01
C28	Munich(Tech. U.)(GERMANY)	22MeV, p,...		0.001
C34	Osaka(RCNP)	80MeV, p,..	k=140	0.0009
C35	Osaka(RCNP)	400MeV, p,..	k=400	0.0002
C39	Tokyo(INS)	45MeV, p,..,h.I.	k=68	0.03
C40	Alma Ata(INP)(KAZAKHSTAN)	30MeV, p,...		
C41	Amsterdam(Vrije U.)(NETHERLANDS)	28MeV, p,...		0.003
C43	Eindhoven(U. of Tech)(NETHERLANDS)	29.5MeV, p,...		
C54	Faure(NAC)(SOUTH AFRICA)	8MeV, p,..		0.0085
C55	Faure(NAC)(SOUTH AFRICA)	8MeV, p,..,h.I.	k=11	0.0085
C56	Faure(NAC)(SOUTH AFRICA)	220MeV, p,.,h.I.	k=220	0.004
C58	Villigen(PSI)(SWITZERLAND)	72MeV, p,...		0.005
C59	Villigen(PSI)(SWITZERLAND)	72MeV, p		0.001
C60	Villigen(PSI)(SWITZERLAND)	590MeV, p		0.001
C61	Kiev(INR-UAS)(UKRAINE)	78MeV, p,..		0.003
C66	Bloomington(IUCF)(UNITED STATES)	205MeV, p,..		0.001
C66	Bloomington(IUCF)(UNITED STATES)	205MeV, p,..		0.001
C69	Davis(U. of Cal.)(UNITED STATES)	68MeV, p,..		0.004
C74	Princeton(U.)(UNITED STATES)	50MeV, p,....		0.0005
C77	Tashkent(NP)(UZBEKISTAN)	22MeV, p,...		0.001

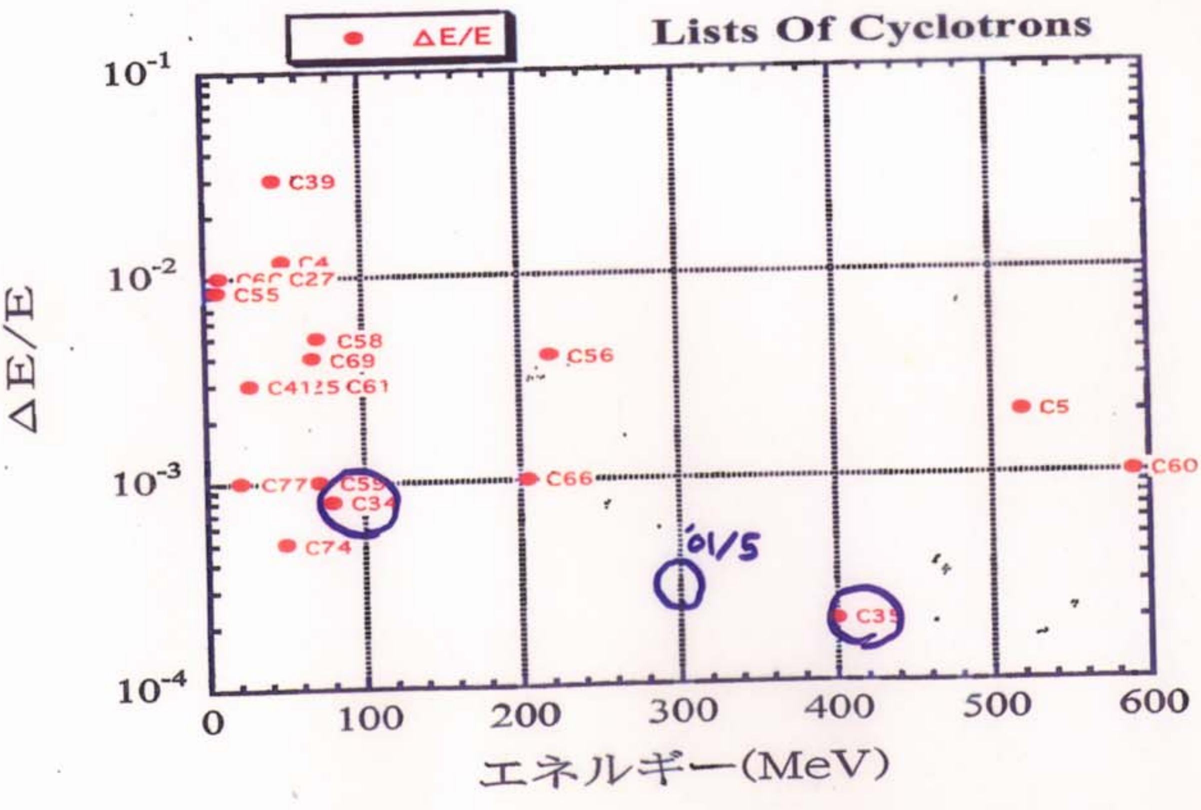

Accelerated Particles (MeV)

H^+……100, 150, 200, 230, 250, 300, 305, 325,
350, 360, 380, 390, 392, 400, 416

D^+……150, 200

H_2^+……185

$^3He^{2+}$…410, 420, 450

$^4He^{2+}$…185, 210, 300, 400

$^6Li^{3+}$…600

$^7Li^{3+}$…455

$^{11}B^{5+}$…786

$^{12}C^{6+}$…480

$^{14}N^{6+}$…910

$^{14}N^{7+}$…560, (980), 1000

$^{16}O^{8+}$…1120

$^{18}O^{8+}$…1080

大阪大学　核物理研究センター
AVFサイクロトロン　更新計画

小型リングサイクロトロン（K=130）の検討

4 SECTOR RING CYCLOTRON
K=130
Focus Limit=70(Ep max=68.5Mev)
Rext=2000mm
Rin=360mm
Bmax=1.65T
Sector Gap=80mm
Trim_Coil=10Sets
Main_Cavity
2 Gap 1/2λ type Vdee=200kV
Frequency(RF)=32~52Mhz
FT_Cavity=Single Gap
Single Gap
Frequency(RF)=96~156MHz Vft=100kV

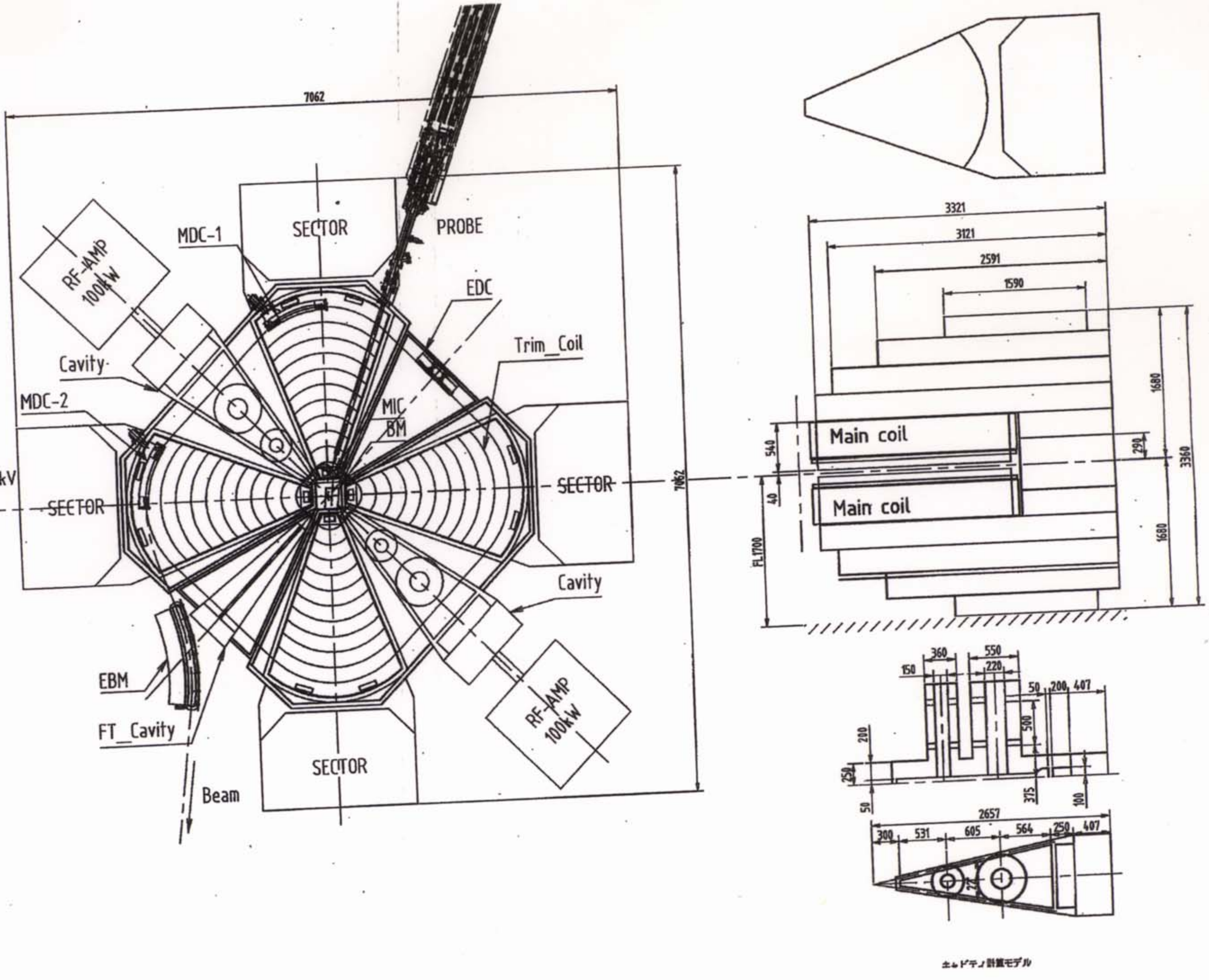

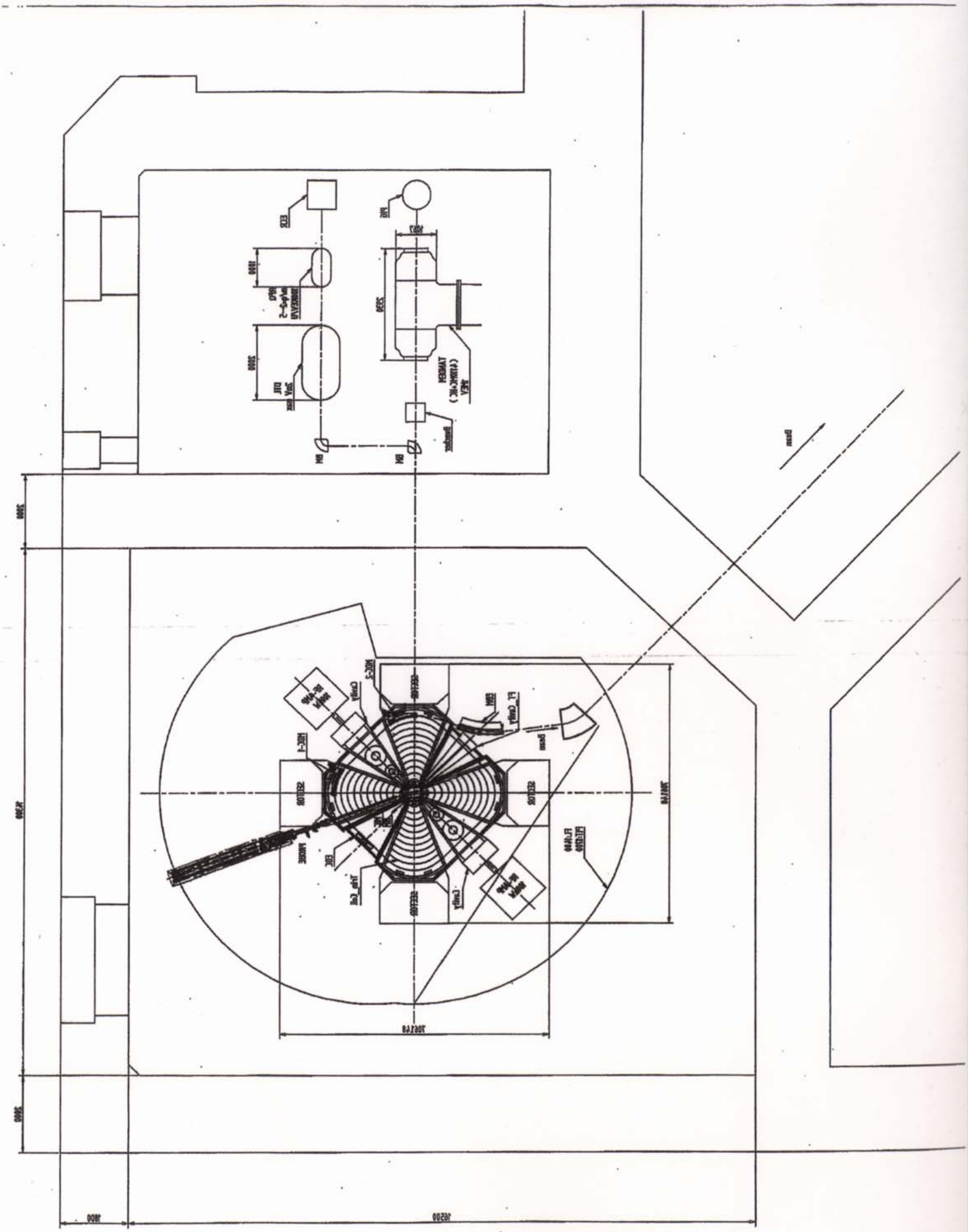

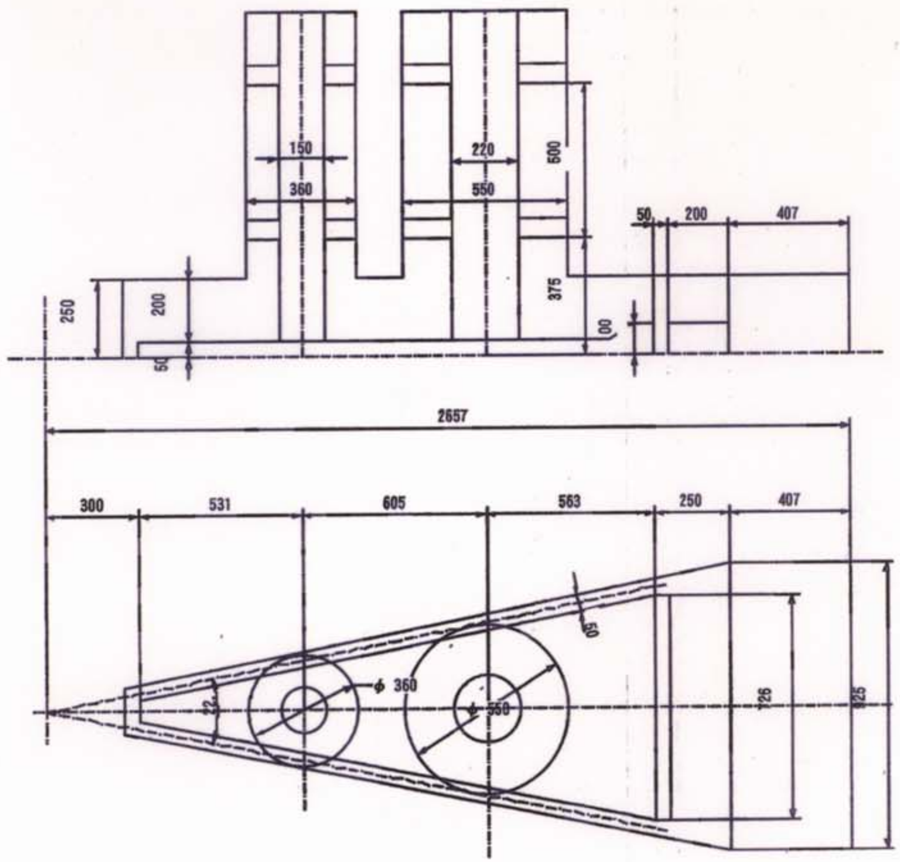

基本仕様

周波数	32～52 MHz
電圧	200 kV
消費電力	100 kW
給電方式	C結合 (50Ω)

Fig.2 :RF加速空洞の概念図

周波数を上げる為、電極の前後に2本の同軸空洞を接続する。

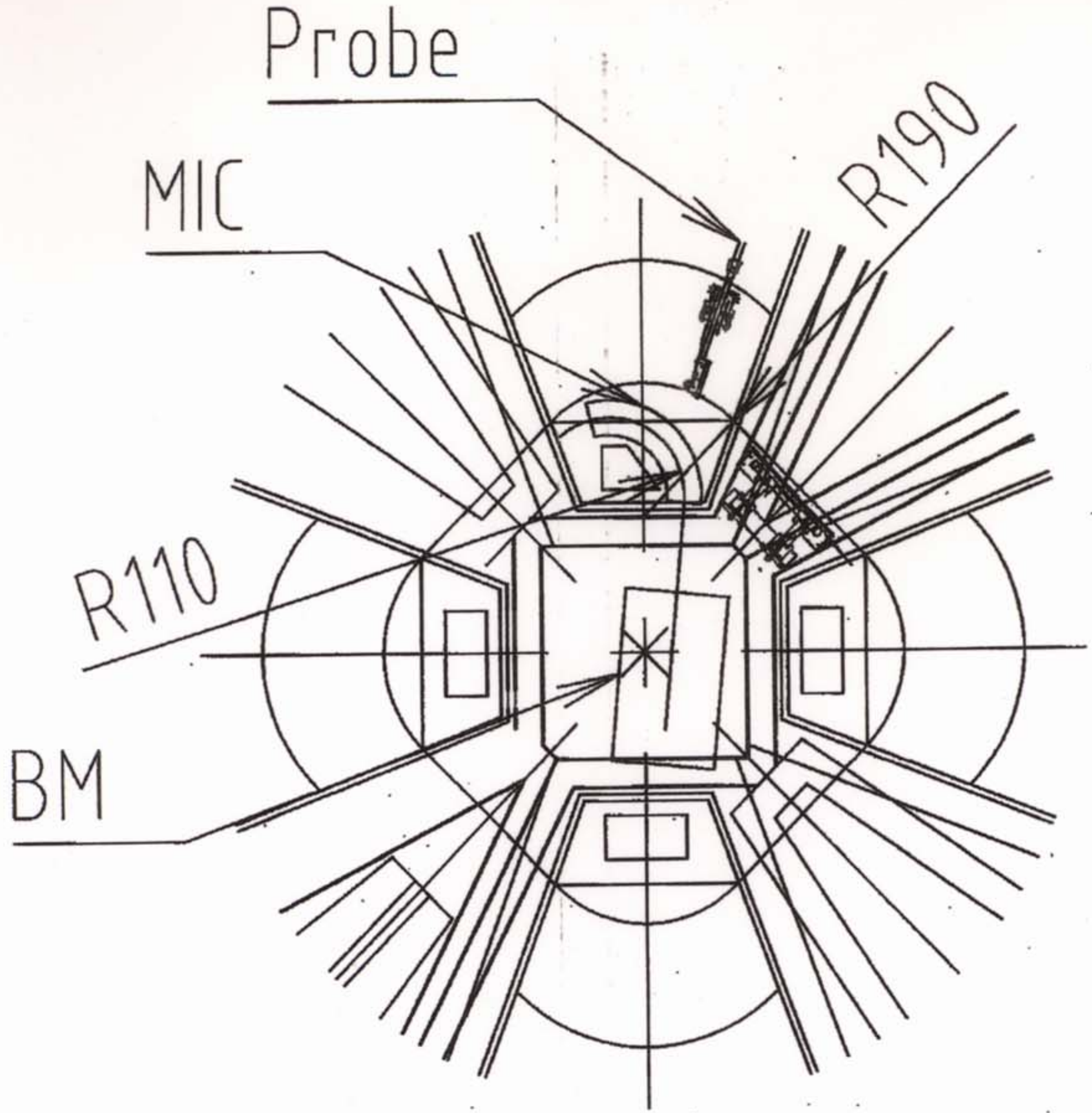

中心領域

表１:小型リングサイクロトロン機器仕様

マグネット	
セクター数	4
スパン角	45 °
最大磁場	1.65 T
磁極ギャップ	80 mm
トリムコイル数	10 組
主コイル起磁力	70,400 AT
主コイル消費電力	kW
トリムコイル電流	300 A
マグネット重量	400 トン
高周波系	
加速系	
加速周波数	32～52 MHz
ギャップ数	4 /turn
最大電圧	200 kV
空胴消費電力	100 kW×2
FT系	
FT周波数	96～156 MHz
ギャップ数	1 /turn
最大電圧	100 kV
空胴消費電力	60 kW

入射系	
静電インフレクタ＋磁気チャネル	
入射平均半径	0.38 m
入射エネルギー	
P	2 MeV
He	1 MeV/U
16O7+	0.89 MeV/U
40Ar12+	0.37 MeV/U
40Ca+10	0.26 MeV/U
引出系	
静電デフレクタ＋磁気チャネル	
引出平均半径	2 m
引出Bρ	1.65 T·m
引出エネルギー	
P	68.5 MeV
He	32.5 MeV/U
16O7+	24.9 MeV/U
40Ar12+	11.7 MeV/U
40Ca+10	8.1 MeV/U

表 2 :低エネルギー入射系の仕様

軽イオン源入射軽

イオン源	PIGタイプ
生成イオン	p、d α
負イオン源	80 mm
タンデトロン加速器	
ターミナル電圧	1 MV
最大電流	100 μA
粒子エネルギー	
p	2 MeV
d	2 MeV
α	3 MeV

重イオン入射系

イオン源	ECRタイプ
周波数	18 GHz
イオン種	C,N,O Ar,Ca
RFQ	
周波数	32-52 MHz
加速エネルギー	100.00 keV/U
電極電圧	35 kV
最大電力	100 kW
電極長さ	1 m
DTL	
周波数	32-52 MHz
加速電圧	2 MV
電極電圧	200 kV
最大電力	200 kW
電極長さ	1.8 m

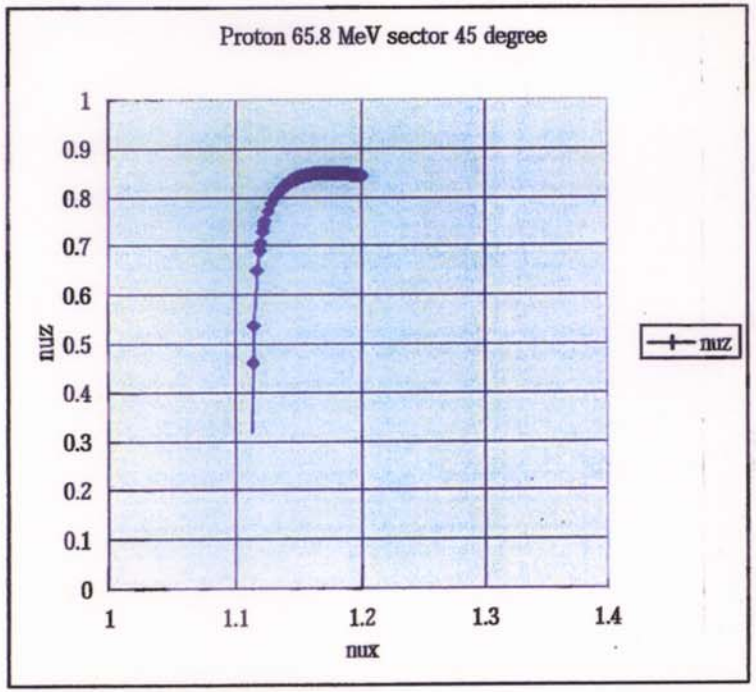

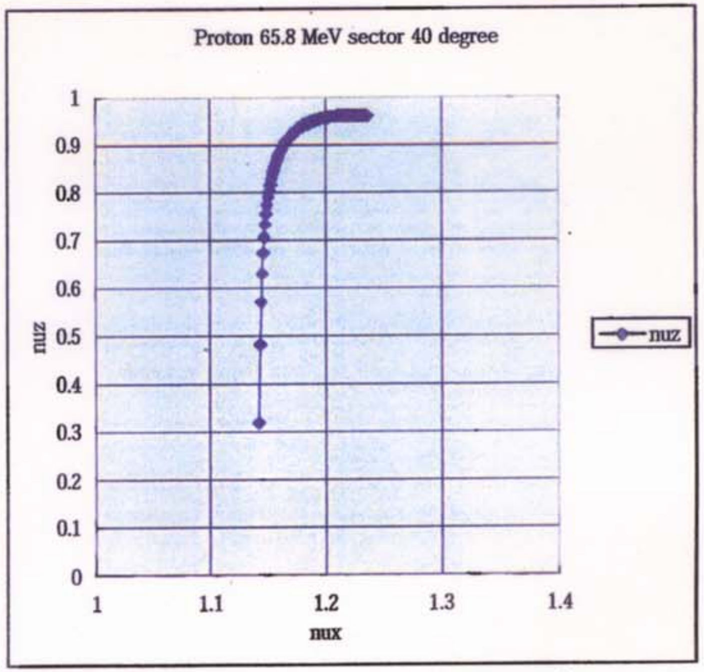

Fig3:セクター角45° と40° のベーターートロン振動 (νz, νr)

45° の場合はνzが、1に近く無いので、共鳴の心配が無い。

表3.1 :リングサイクロトロンの運転パラメーター(K=130)

平均半径(m)	MeV/u	gamma	beta	Freq(MHz)	RF Freq(MHz	harmonics
2	68.5	0.07302772	0.36260641	8.66	51.94	6
2	50	0.0533049	0.31409151	7.50	44.99	6
2	24.2	0.02579957	0.22286506	5.32	31.92	6
2	35	0.03731343	0.26579789	6.35	50.77	8
2	13	0.01385928	0.164781	3.93	31.47	8
2	9	0.00959488	0.13753935	3.28	32.84	10

K= 130 sector angle= 45.00

	extraction					Injection				
核種	p	4He2+	16O7+	40Ar12+	40Ca+10	p	4He2+	16O7+	40Ar12+	40Ca+10
M/Q	1.000	2.000	2.286	3.333	4.000	1.000	2.000	2.286	3.333	4.000
平均半径(m)	2	2	2	2	2	0.36	0.36	0.36	0.36	0.36
MeV/u	68.5	32.5	24.9	11.7	8.1	2.00	1.00	0.78	0.37	0.26
gamma	0.074	0.035	0.027	0.013	0.009	0.002	0.001	0.001	0.000	0.000
beta	0.364	0.258	0.227	0.157	0.131	0.065	0.046	0.041	0.028	0.024
Freq(MHz)	8.69	6.15	5.41	3.75	3.13	8.69	6.14	5.41	3.75	3.13
RF Freq(MHz)	52.12	36.89	32.47	37.50	31.34	52.12	36.85	32.47	37.50	31.34
harmonics	6	6	6	10	10	6	6	6	10	10
$\sqrt{1-B2}$	0.93	0.97	0.97	0.99	0.99	1.00	1.00	1.00	1.00	1.00
B* ρ (T*m)	1.21	1.65	1.65	1.65	1.64	0.20	0.29	0.29	0.29	0.29
B(average)	0.61	0.83	0.83	0.82	0.82	0.57	0.80	0.80	0.81	0.81
ρ (m)	1	1	1	1	1	0.18	0.18	0.18	0.18	0.18
B(T)	1.21	1.65	1.65	1.65	1.64	1.13	1.60	1.61	1.63	1.63
B ρ β	0.441	0.426	0.374	0.258	0.216	0.013	0.013	0.012	0.008	0.007
M0(MeV)	931	931	931	931	931	931	931	931	931	931
C(1E6 m/sec)	3.00E+02	3.00E+02	3.00E+02	3.00E+02	3.00E+02	3.00E+02	3.00E+02	3.00E+02	3.00E+02	3.00E+02

表3.2:リングサイクロトロンの運転パラメーター

K=150 参考)磁場が強すぎる

平均半径(m)	平均半径(m)	MeV/u	gamma	beta	Freq(MHz)	RF Freq(MHz	harmonics
2	2	68.5	0.07302772	0.36260641	8.66	51.94	6
2	2	50	0.0533049	0.31409151	7.50	44.99	6
2	2	24.2	0.02579957	0.22286506	5.32	31.92	6
2	2	35	0.03731343	0.26579789	6.35	50.77	8
2	2	13	0.01385928	0.164781	3.93	31.47	8
2	2	9	0.00959488	0.13753935	3.28	32.84	10

K= 150 sector angle= 45.00

	extraction						Injection				
核種	p	4He2+	16O7+	40Ar12+	40Ca+10	核種	p	4He2+	16O7+	40Ar12+	40Ca+10
M/Q	1.000	2.000	2.286	3.333	4.000	M/Q	1.000	2.000	2.286	3.333	4.000
平均半径(m)	2	2	2	2	2	平均半径(m)	0.36	0.36	0.36	0.36	0.36
MeV/u	68.5	37.5	28.7	13.5	9.4	MeV/u	2.00	1.15	0.89	0.43	0.30
gamma	0.074	0.040	0.031	0.015	0.010	gamma	0.002	0.001	0.001	0.000	0.000
beta	0.364	0.276	0.243	0.168	0.141	beta	0.065	0.050	0.044	0.030	0.025
Freq(MHz)	8.69	6.58	5.80	4.02	3.36	Freq(MHz)	8.69	6.59	5.80	4.03	3.36
RF Freq(MHz)	52.12	39.47	34.78	32.18	33.63	RF Freq(MHz	52.12	39.52	34.77	32.24	33.63
harmonics	6	6	6	8	10	harmonics	6	6	6	8	10
√1-B2	0.93	0.96	0.97	0.99	0.99	√1-B2	1.00	1.00	1.00	1.00	1.00
B*ρ (T*m)	1.21	1.78	1.78	1.77	1.77	B*ρ (T*m)	0.20	0.31	0.31	0.31	0.31
B(average)	0.61	0.89	0.89	0.88	0.88	B(average)	0.57	0.86	0.86	0.87	0.87
ρ (m)	1	1	1	1	1	ρ (m)	0.18	0.18	0.18	0.18	0.18
B(T)	1.21	1.78	1.78	1.77	1.77	B(T)	1.13	1.71	1.72	1.75	1.75
Bρβ	0.441	0.490	0.431	0.298	0.249	Bρβ	0.013	0.015	0.014	0.010	0.008
M0(MeV)	931	931	931	931	931	M0(MeV)	931	931	931	931	931
C(1E6 m/sec)	3.00E+02	3.00E+02	3.00E+02	3.00E+02	3.00E+02	C(1E6 m/sec	3.00E+02	3.00E+02	3.00E+02	3.00E+02	3.00E+02

小型リングサイクロの問題点

1. 入射半径が小さい為、磁場強度を1. 5T程度にしか出来ない。

2. 中心部が狭い為に、超伝導コイル用のクライオスタットのスペースが確保できない。

3. FT空洞の中心部は、電圧がかからない。

4. 真空箱の分割方法が複雑になる。

大阪大学　核物理研究センター

AVFサイクロトロン　更新計画

超伝導小型リングサイクロトロン（K=130）

図2 超伝導小型リングサイクロトロン平面図

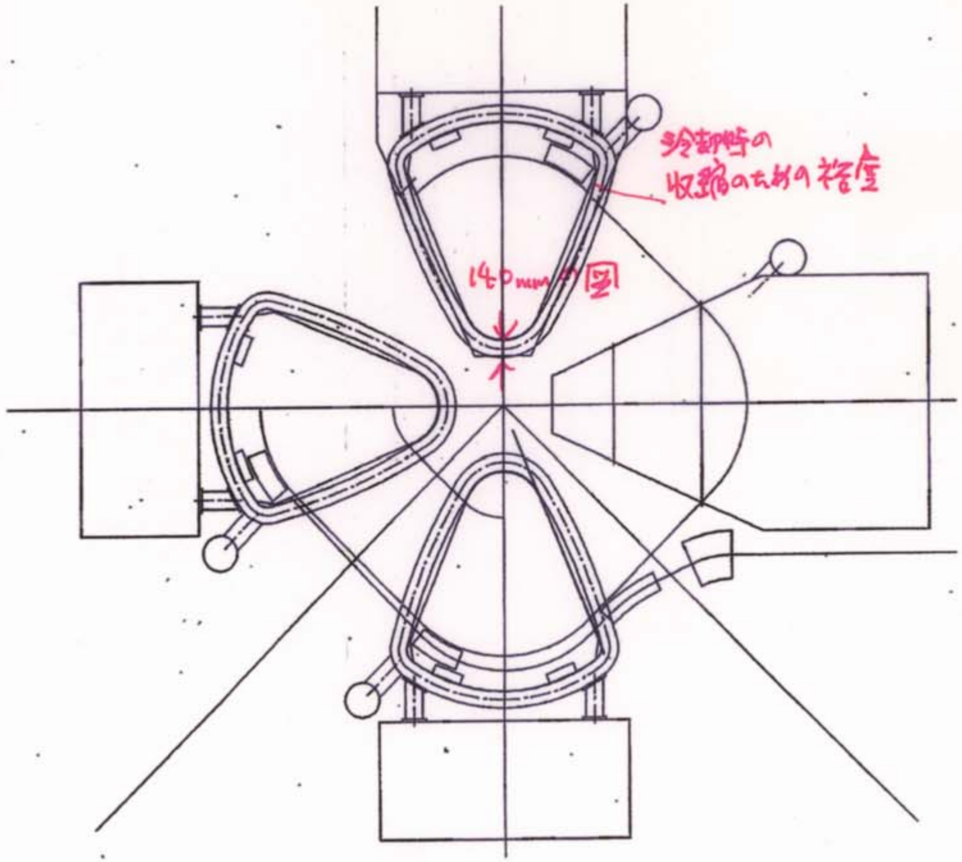

	常伝導	超伝導
入射半径 $\bar{R}$	0.38m	0.95m
取出し半径	2m	2m

図1　超伝導コイル断面図

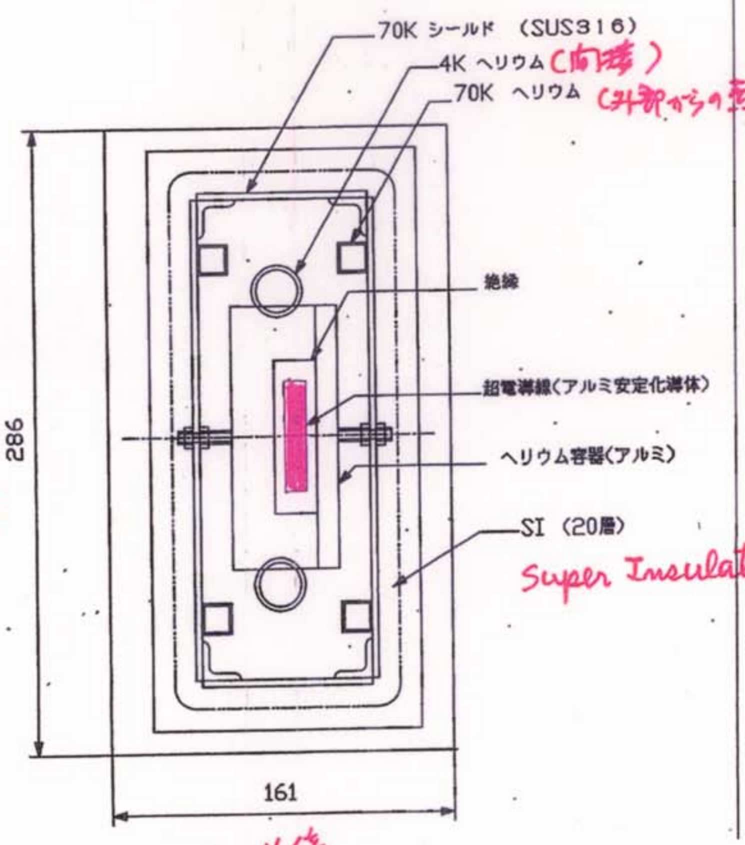

02/02/25

表1：超伝導小型リングサイクロトロン機器仕様

マグネット		
	セクター数	4
	スパン角	45°
	最大磁場	1.65T
	磁極ギャップ	80mm
	トリムコイル数	10組
	主コイル起磁力	70, 400AT
	トリムコイル電流	300A
	マグネット 重量	400ton
高周波系		
加速系		
	加速周波数	32-52MHz
	ギャップ数	4/turn
	最大電圧	200kV
	空洞消費電力	100kW×2
FT系		
	FT周波数	96-156MHz
	ギャップ数	1/turn
	最大電圧	100kV
	空洞消費電力	60kW

入射系			
	静電インフレクター＋磁気チャネル		
	入射平均半径	0.95m	
	入射エネルギー		
	p	14.2MeV/n	2MeV
	α	7.1MeV/n	1MeV/u
	$^{16}O^{7+}$	5.4MeV/n	0,89 MeV/u
	$^{40}Ar^{12+}$	2.6MeV/n	0,37
	$^{40}Ca^{10+}$	1.8MeV/n	0,26
引出系			
	静電インフレクター＋磁気チャネル		
	~~入射~~引出平均半径	~~0.95m~~ 2m	
	引出B ρ	1.65T	
	入射エネルギー		
	p	68.5MeV/n	
	α	32.5MeV/n	
	$^{16}O^{7+}$	24.9MeV/n	
	$^{40}Ar^{12+}$	11.7MeV/n	
	$^{40}Ca^{10+}$	8.1MeV/n	

表2：低エネルギー入射系の仕様

軽イオン入射系

イオン源形式	PI Gタイプ
生成イオン	p、d
前段加速器形式	タンデム
ターミナル電圧	7.5MV
粒子エネルギー	
p	15MeV
d	7.5MeV/n
α	5.6MeV/n ← 7.1 MeV/u

1MV
2MeV

重イオン入射系

ECRイオン源	
周波数	18GHz
イオン種	α, C, O, Ar, Ca
RFQ	
周波数	32-52MHz
加速エネルギー	100keV/n
電極電圧	35kV
最大電力	100kW
電極長さ	1m
DTL	
周波数	32-52MHz
加速電圧	15MV
電極電圧	200kV
最大電力	～1200kW
電極長さ	～40m

中小型化

あるいは

K＝30 小型サイクロトロン

p	30MeV
d	15MeV
α	7.5MeV/n
$^{16}O^{7+}$	5.7MeV/n
$^{40}Ar^{12+}$	2.7MeV/n
$^{40}Ca^{10+}$	1.9MeV/n

垂直入射

表3 超伝導小型リングサイクロトロンの運転パラメータ

平均半径(m)	MeV/u	gamma	beta	Freq(MHz)	RF Freq(MHz)	harmonics
2	68.5	0.07302772	0.36260641	8.66	51.94	6
2	50	0.0533049	0.31409151	7.50	44.99	6
2	25	0.02665245	0.22637829	5.40	32.43	6
2	12	0.01279318	0.15844116	3.78	22.70	6
2	6.8	0.00724947	0.11976135	2.86	17.16	6
2	2.5	0.00266525	0.07286464	1.74	10.44	6

K= 130 sector 45.00

	extraction				
核種	p	4He2+	16O7+	40Ar12+	40Ca10+
M/Q	1.000	2.000	2.286	3.333	4.000
平均半径(m)	2	2	2	2	2
MeV/u	68.5	32.5	24.9	11.7	8.1
gamma	0.074	0.035	0.027	0.013	0.009
beta	0.364	0.258	0.227	0.157	0.131
Freq(MHz)	8.69	6.15	5.41	3.75	3.13
RF Freq(MHz)	52.12	36.89	32.47	37.50	31.34
harmonics	6	6	6	10	10
√1-B2	0.93	0.97	0.97	0.99	0.99
B*ρ(T*m)	1.21	1.65	1.65	1.65	1.64
B(average)	0.61	0.83	0.83	0.82	0.82
ρ(m)	1	1	1	1	1
B(T)	1.21	1.65	1.65	1.65	1.64
Bρβ	0.441	0.426	0.374	0.258	0.216
M0(MeV)	931	931	931	931	931
C(1E6 m/sec)	3.00E+02	3.00E+02	3.00E+02	3.00E+02	3.00E+02

	Inj				
核種	p	4He2+	16O7+	40Ar12+	40Ca10+
M/Q	1.000	2.000	2.286	3.333	4.000
平均半径(m)	0.95	0.95	0.95	0.95	0.95
MeV/u	14.24	7.05	5.44	2.60	1.81
gamma	0.015	0.008	0.006	0.003	0.002
beta	0.173	0.122	0.108	0.075	0.062
Freq(MHz)	8.69	6.15	5.41	3.75	3.13
RF Freq(MHz)	52.14	36.90	32.46	37.50	31.31
harmonics	6	6	6	10	10
√1-B2	0.98	0.99	0.99	1.00	1.00
B*ρ(T*m)	0.54	0.77	0.77	0.77	0.77
B(average)	0.57	0.81	0.81	0.81	0.82
ρ(m)	0.18	0.18	0.18	0.18	0.18
B(T)	3.03	4.25	4.27	4.30	4.30
Bρβ	0.094	0.094	0.083	0.058	0.048
M0(MeV)	931	931	931	931	931
C(1E6 m/sec)	3.00E+02	3.00E+02	3.00E+02	3.00E+02	3.00E+02

02/02/25

大阪大学　核物理研究センター
入射加速器　更新計画

Hybridサイクロトロンの検討

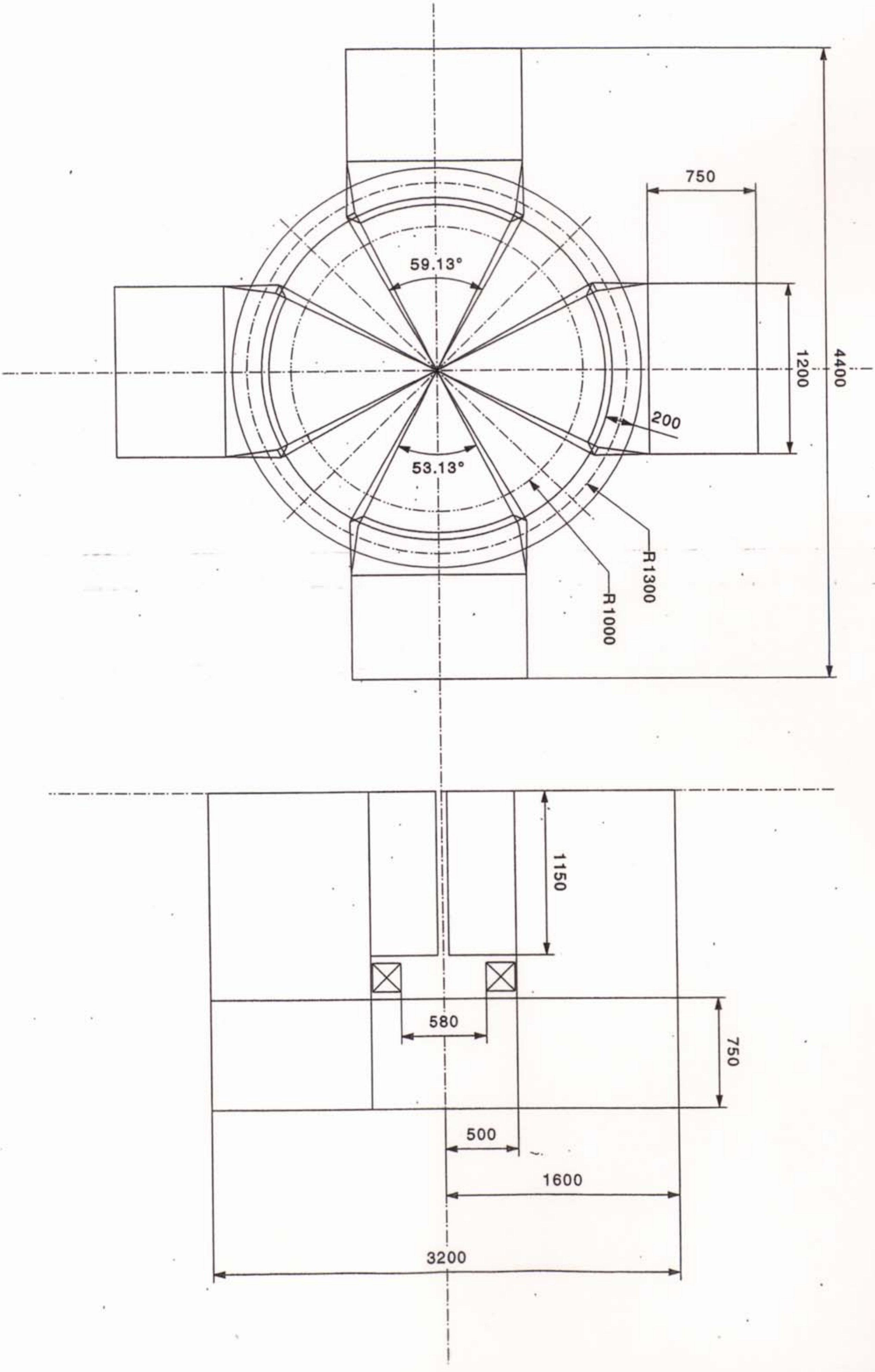

750
59.13°
1200
4400
200
53.13°
R1300
R1000
1150
580
750
500
1600
3200

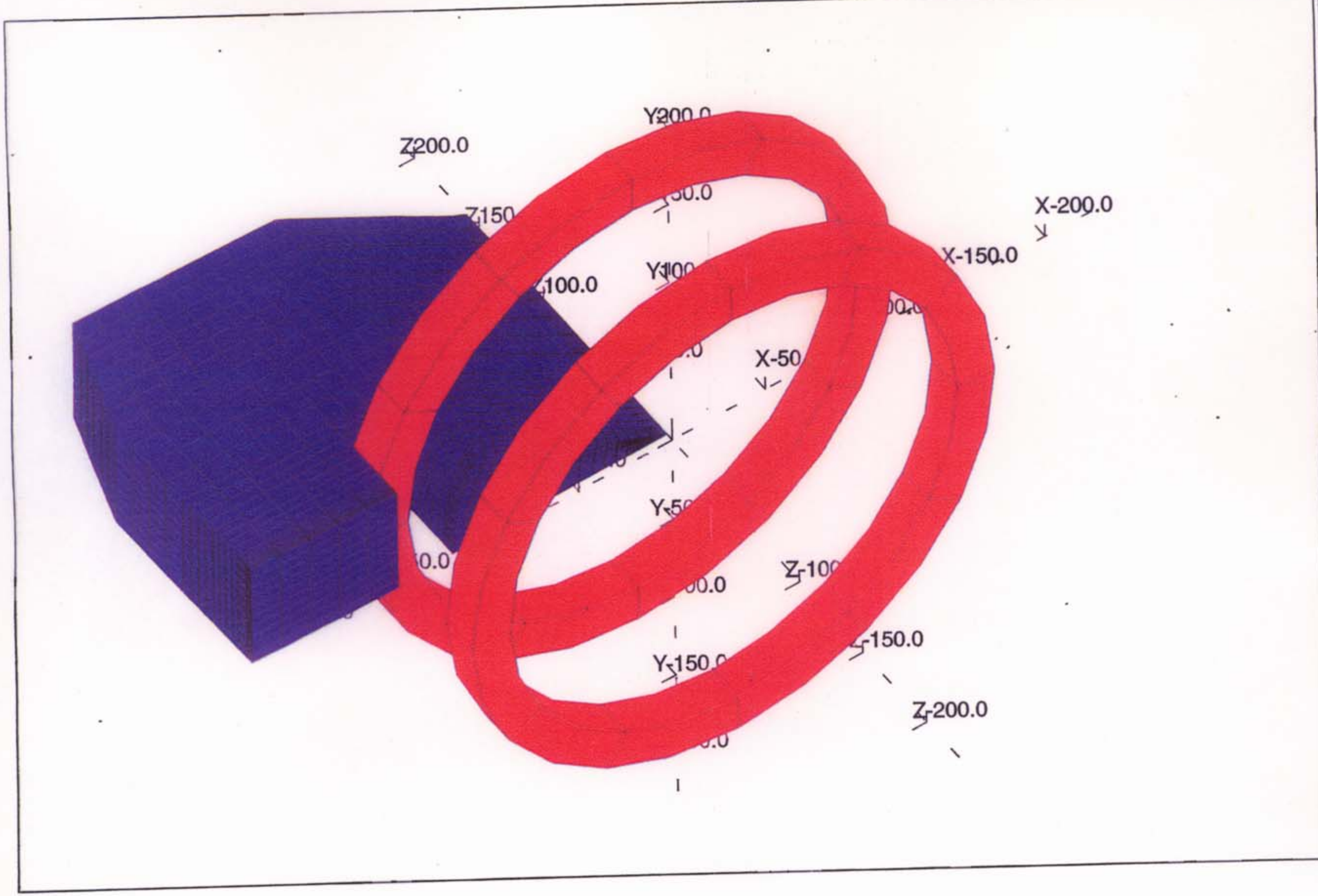

UNITS

Length	: cm
Magn Flux Den	: gauss
Magnetic field	: oersted
Magn Scalar Pot	: oersted-cm
Magn Vector Pot	: gauss-cm
Elec Flux Den	: C cm^{-2}
Electric field	: V cm^{-1}
Conductivity	: S cm^{-1}
Current density	: A cm^{-2}
Power	: W
Force	: N
Energy	: J

PROBLEM DATA
saka/hyb/y12a200.op3
TOSCA
Magnetostatic
Non-linear materials
Simulation No 1 of 1
19500 elements
28965 nodes
Nodal fields

LOCAL COORDS.

Xlocal	= 0.0
Ylocal	= 0.0
Zlocal	= 0.0
Theta	= 0.0
Phi	= 0.0
Psi	= 0.0

14/Mar/2002 09:54:36 Page 5

OPERA-3d
Post-Processor 7.1

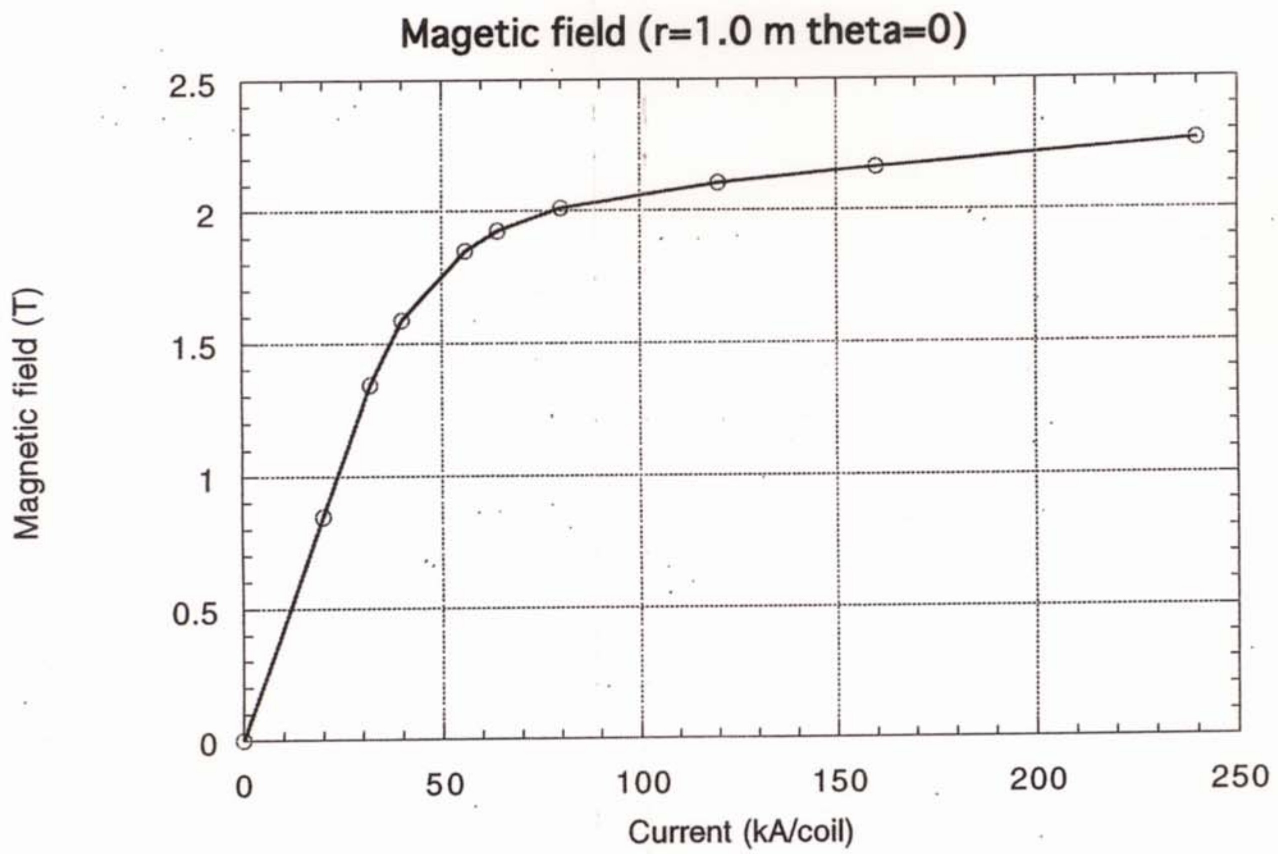
Magetic field (r=1.0 m theta=0)
Magnetic field (T)
0
0.5
1
1.5
2
2.5
0
50
100
150
200
250
Current (kA/coil)

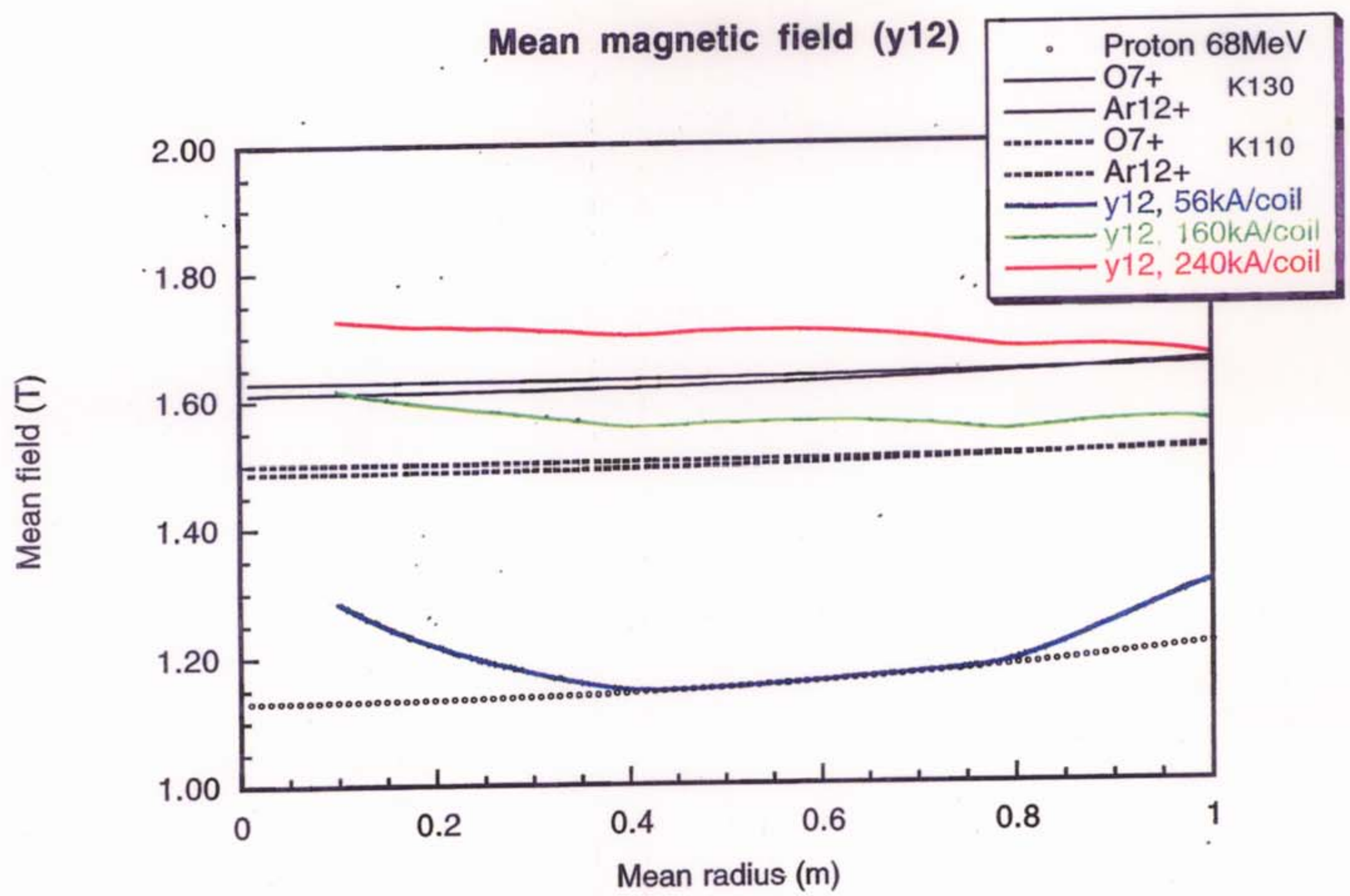
Mean magnetic field (y12)
Proton 68MeV
O7+
K130
Ar12+
O7+
K110
Ar12+
y12, 56kA/coil
y12, 160kA/coil
y12, 240kA/coil
2.00
1.80
1.60
1.40
1.20
1.00
Mean field (T)
0
0.2
0.4
0.6
0.8
1
Mean radius (m)

Magnetic field distribution (r=0.25 m)

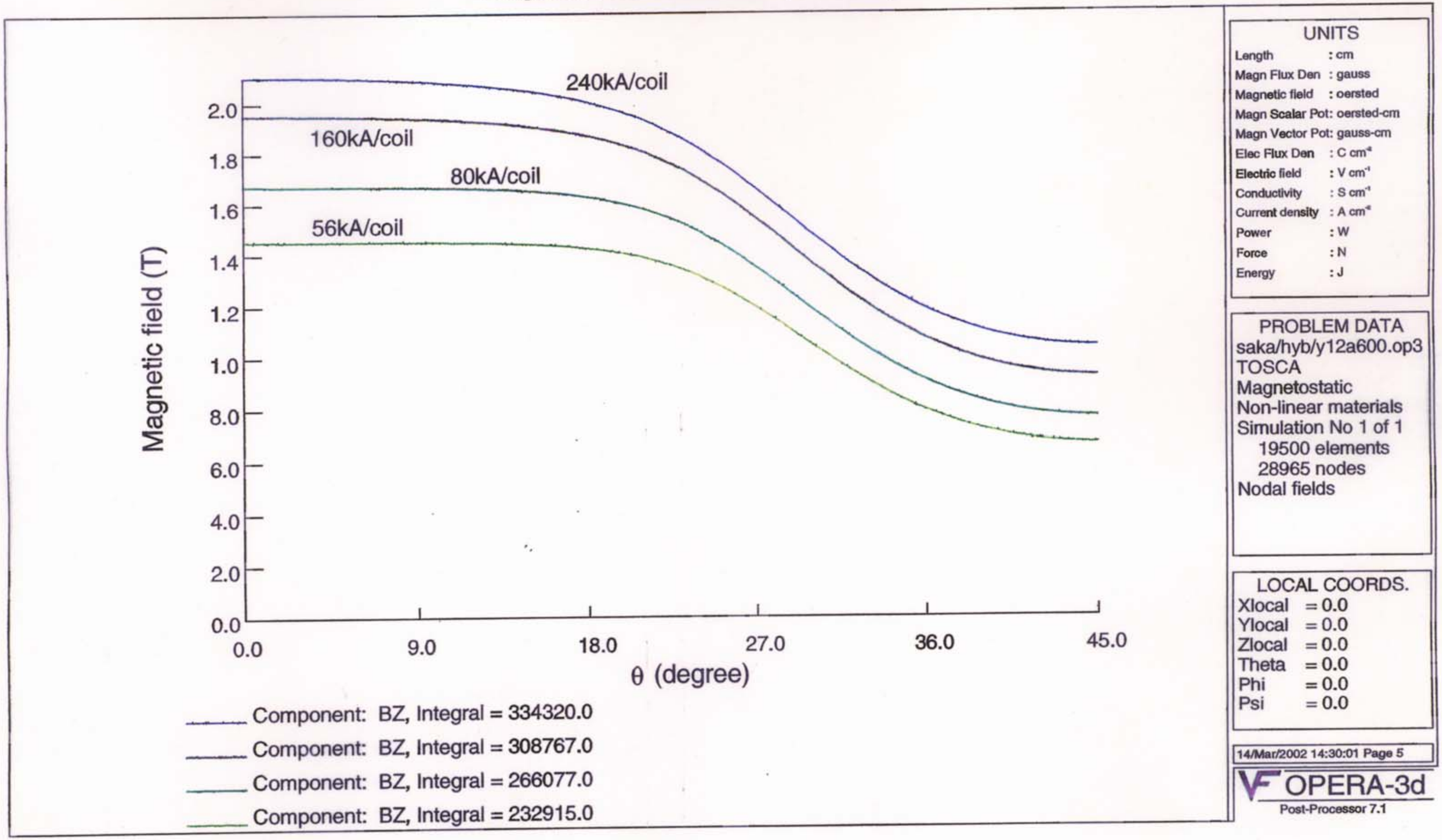

Magnetic field distribution (r=1.0 m)

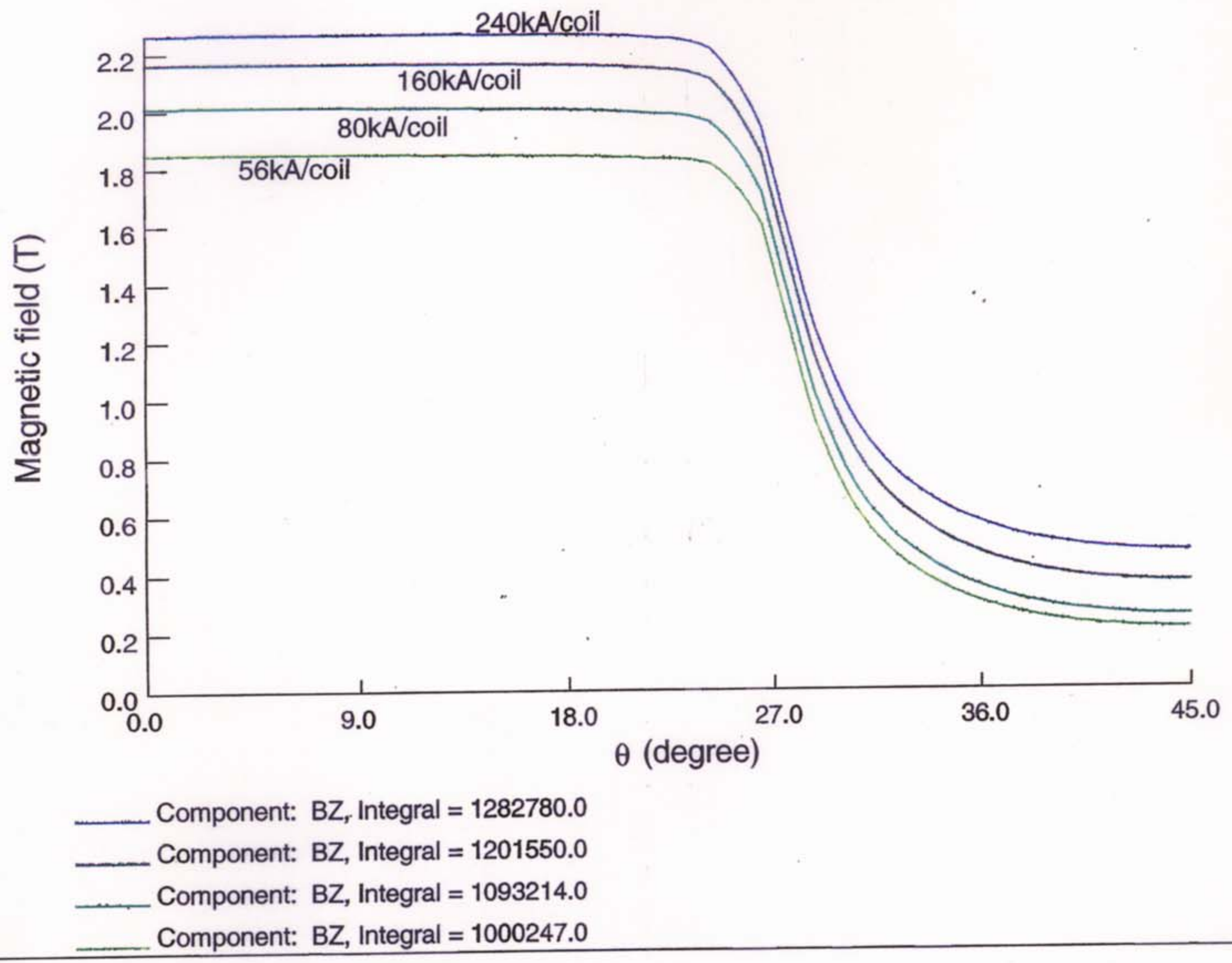

UNITS

Length	: cm
Magn Flux Den	: gauss
Magnetic field	: oersted
Magn Scalar Pot	: oersted-cm
Magn Vector Pot	: gauss-cm
Elec Flux Den	: C cm^{-2}
Electric field	: V cm^{-1}
Conductivity	: S cm^{-1}
Current density	: A cm^{-2}
Power	: W
Force	: N
Energy	: J

PROBLEM DATA
hyb/y12a600.op3
TOSCA
Magnetostatic
Non-linear materials
Simulation No 1 of 1
19500 elements
28965 nodes
Nodal fields

LOCAL COORDS.
Xlocal = 0.0
Ylocal = 0.0
Zlocal = 0.0
Theta = 0.0
Phi = 0.0
Psi = 0.0

14/Mar/2002 13:32:30 Page 4

OPERA-3d
Post-Processor 7.1

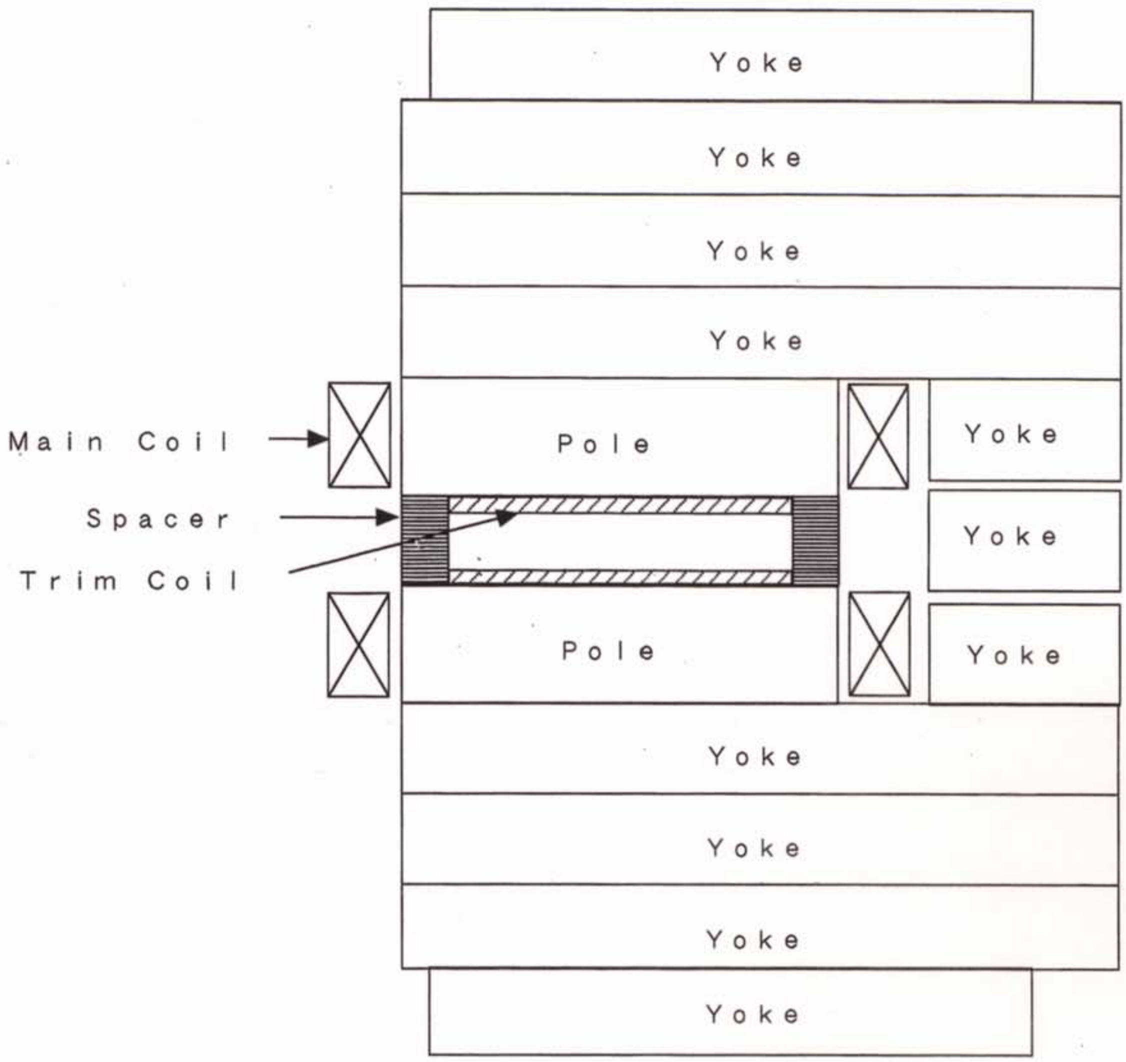

Structure of the Sector Magnet for the Ring Cyclotron

GANIL SPIRAL CIME

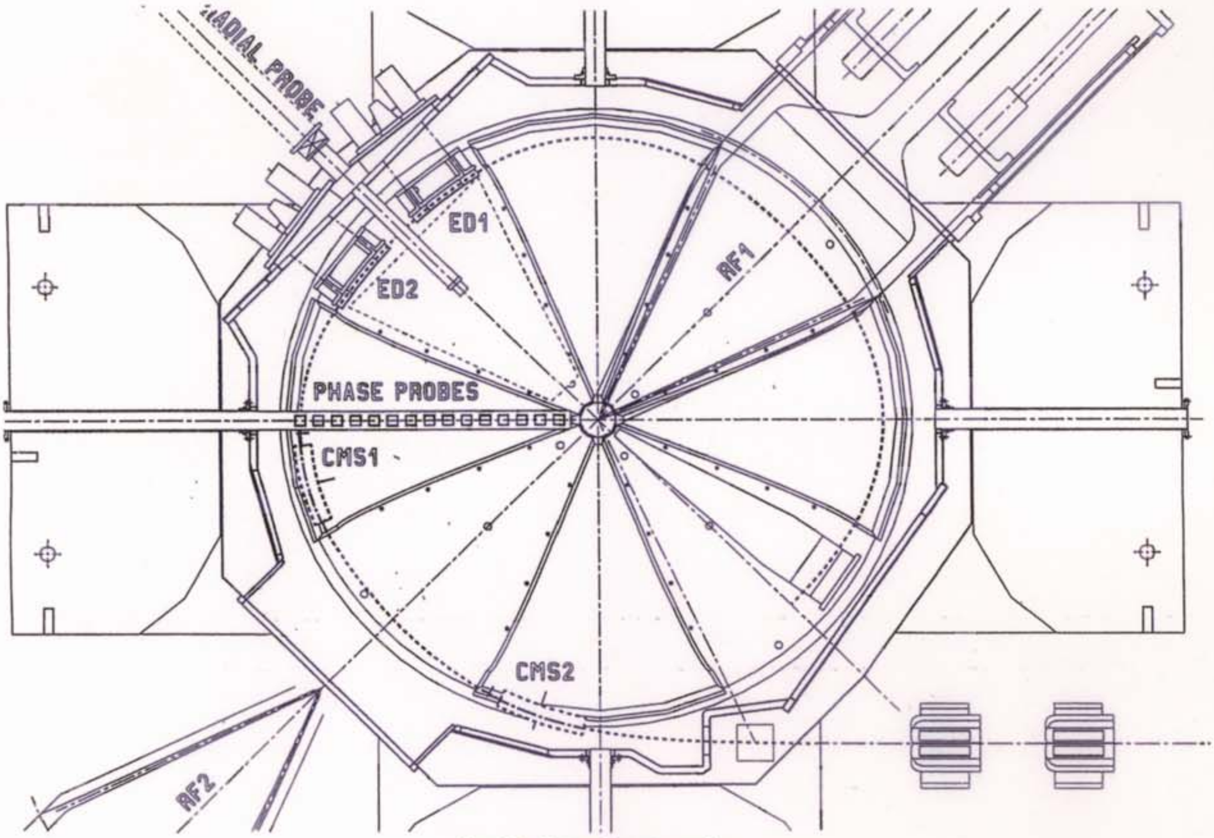

Fig. 10 : Extraction elements

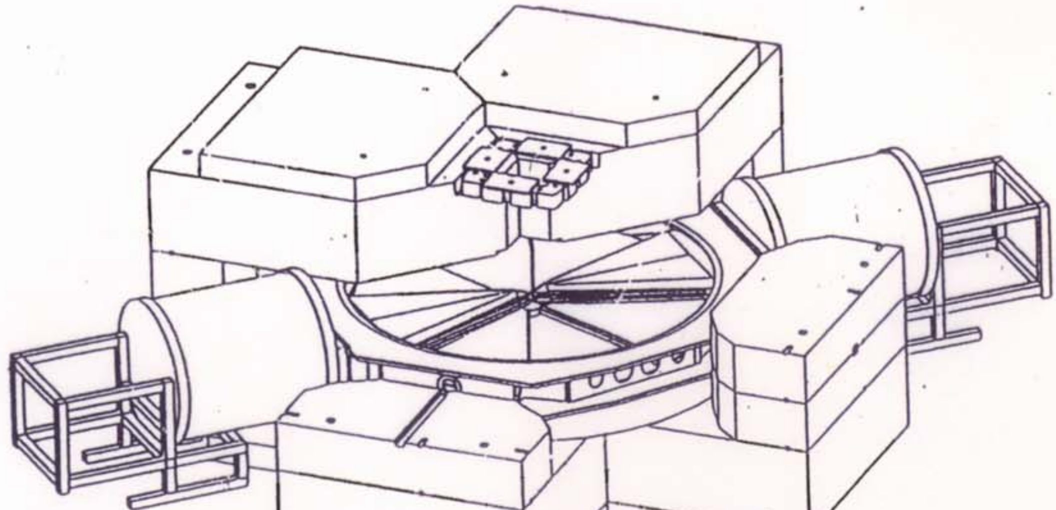

Fig. 8 : Magnet structure

大阪大学　核物理研究センター

入射加速器　更新計画

AVFサイクロトロン（K=130）の検討

2002年3月5日

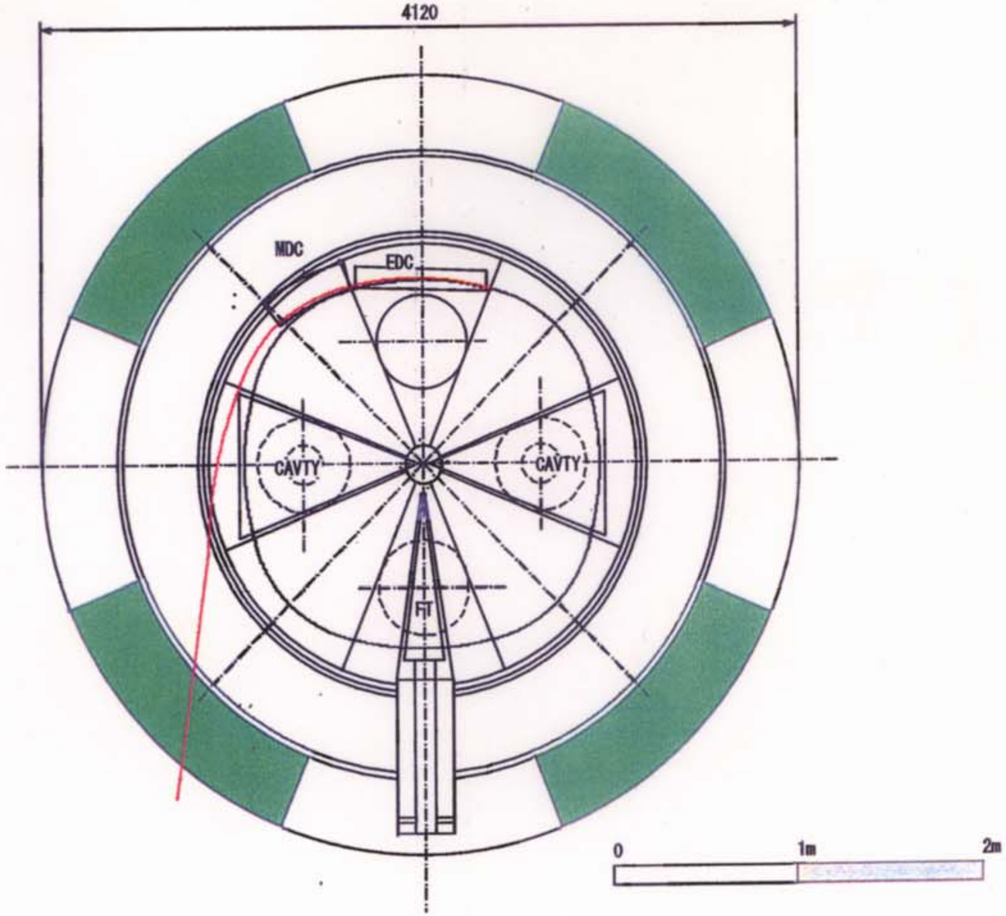

図1：AVFサイクロトロン平面図

2002年3月5日

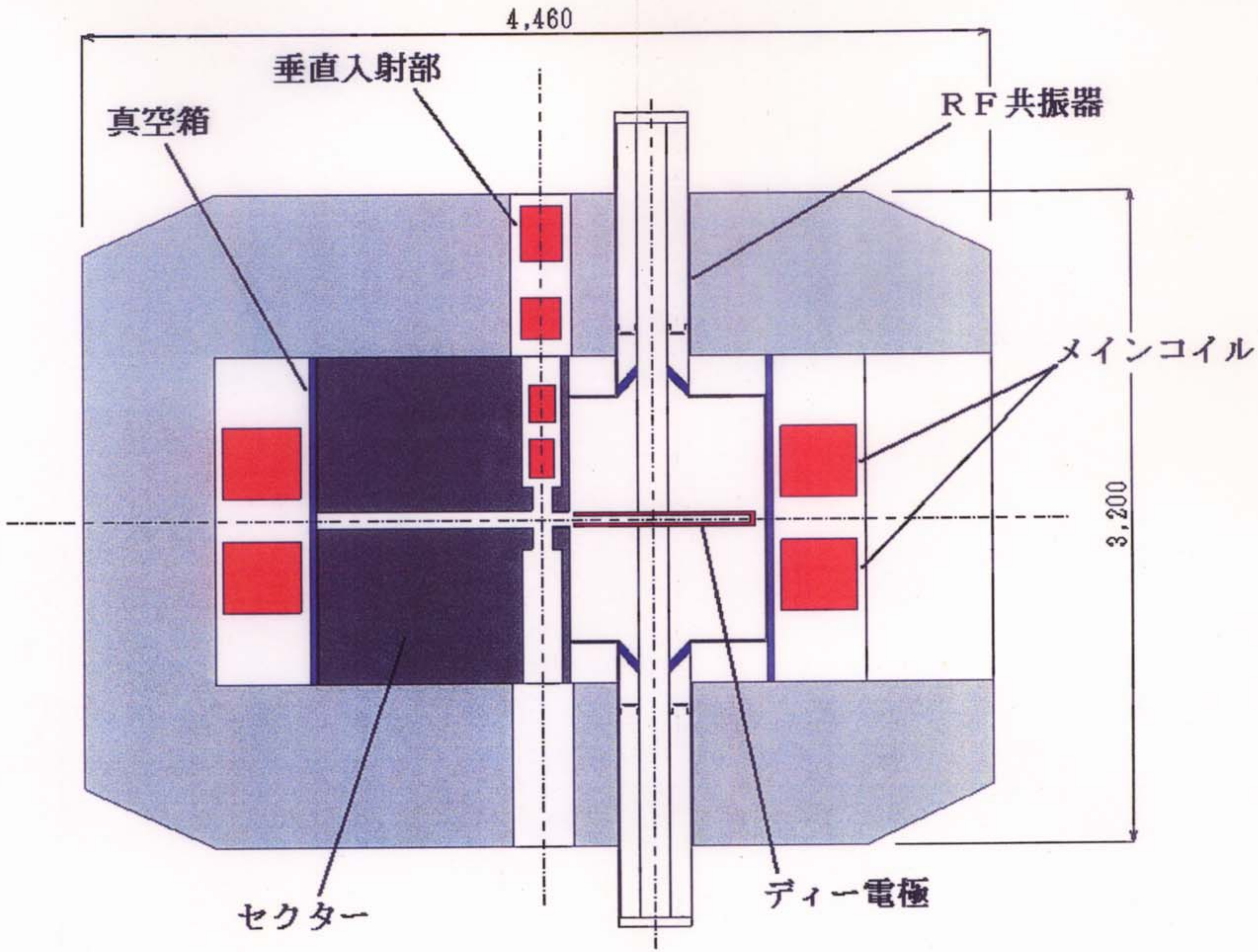
4,460
垂直入射部
真空箱
ＲＦ共振器
メインコイル
3,200
ディー電極
セクター

表1：AVFサイクロトロン(K=130)機器仕様

マグネット	
セクター数	4
スパン角	45°
ヒル／バレー磁場	2/1T
磁極ギャップ	80mm
トリムコイル数	10組
主コイル起磁力	600,000AT
主コイル消費電力	250kW
トリムコイル電流	300A
マグネット重量	200ton
高周波系	
加速系	
加速周波数	32-52MHz
ギャップ数	4/turn
最大電圧	200kV
空洞消費電力	100kW×2
ＦＴ系	
ＦＴ周波数	96-156MHz
ギャップ数	1/turn
最大電圧	100kV
空洞消費電力	60kW

入射系		
静電スパイラルインフレクター		
入射平均半径		30mm
入射エネルギー		
	p	55keV/n
	α	28keV/n
	$^{16}O^{7+}$	22keV/n
	$^{40}Ar^{12+}$	10keV/n
	$^{40}Ca^{10+}$	7eV/n
引出系		
静電インフレクター＋磁気チャネル		
引出平均半径		1m
引出Ｂρ		1.65T・m
引出エネルギー		
	p	68.5MeV/n
	α	32.5MeV/n
	$^{16}O^{7+}$	24.9MeV/n
	$^{40}Ar^{12+}$	11.7MeV/n
	$^{40}Ca^{10+}$	8.1MeV/n

2002年3月5日

表2:低エネルギー入射系の仕様

軽イオン入射系

イオン源形式	マルチカスプ
生成イオン	p、d
引出電圧	60kV

重イオン入射系

ＥＣＲイオン源	
周波数	18GHz
引出電圧	60kV
最大電流	100 μ A
イオン種	α, C, O, Ar, Ca

表3　AVFサイクロトロンの運転パラメター(K=130)

平均半径(m)	MeV/u	gamma	beta	Freq(MHz)	RF Freq(MHz)	harmonics
1	68.5	0.07302772	0.36260641	17.31	51.94	3
1	50	0.0533049	0.31409151	15.00	44.99	3
1	25	0.02665245	0.22637829	10.81	32.43	3
1	12	0.01279318	0.15844116	7.57	22.70	3
1	6.8	0.00724947	0.11976135	5.72	22.87	4
1	2.5	0.00266525	0.07286464	3.48	13.92	4

K=　130　sector　45.00

	extraction						Inj				
核種	p	4He2+	16O7+	40Ar12+	40Ca10+	核種	p	4He2+	16O7+	40Ar12+	40Ca10+
M/Q	1.000	2.000	2.286	3.333	4.000	M/Q	1.000	2.000	2.286	3.333	4.000
平均半径(m)	1	1	1	1	1	平均半径(m)	0.03	0.03	0.03	0.03	0.03
MeV/u	68.5	32.5	24.9	11.7	8.1	MeV/u	0.055	0.028	0.022	0.010	0.007
gamma	0.074	0.035	0.027	0.013	0.009	gamma	0.000	0.000	0.000	0.000	0.000
beta	0.364	0.258	0.227	0.157	0.131	beta	0.011	0.008	0.007	0.005	0.004
Freq(MHz)	17.37	12.30	10.82	7.50	6.27	Freq(MHz)	17.37	12.30	10.82	7.50	6.27
RF Freq(MHz)	52.12	36.89	32.47	37.50	31.34	RF Freq(MHz	52.11	36.90	32.46	37.50	31.35
harmonics	3	3	3	5	5	harmonics	3	3	3	5	5
√1-B2	0.93	0.97	0.97	0.99	0.99	√1-B2	1.00	1.00	1.00	1.00	1.00
B*ρ (T*m)	1.21	1.65	1.65	1.65	1.64	B*ρ (T*m)	0.03	0.05	0.05	0.05	0.05
B(average)	1.21	1.65	1.65	1.65	1.64	B(average)	1.13	1.60	1.61	1.62	1.63
ρ (m)	1	1	1	1	1	ρ (m)	0.03	0.03	0.03	0.03	0.03
B(T)	1.21	1.65	1.65	1.65	1.64	B(T)	1.13	1.60	1.61	1.62	1.63
Bρβ	0.441	0.426	0.374	0.258	0.216	Bρβ	0.000	0.000	0.000	0.000	0.000
M0(MeV)	931	931	931	931	931	M0(MeV)	931	931	931	931	931
C(1E6 m/sec)	3.00E+02	3.00E+02	3.00E+02	3.00E+02	3.00E+02	C(1E6 m/sec)	3.00E+02	3.00E+02	3.00E+02	3.00E+02	3.00E+02
						Vinj (kV)	55.4	55.6	49.2	34.5	28.9

2002年3月5日

図.2: AVFサイクロトロンの加速可能範囲 (K=130)

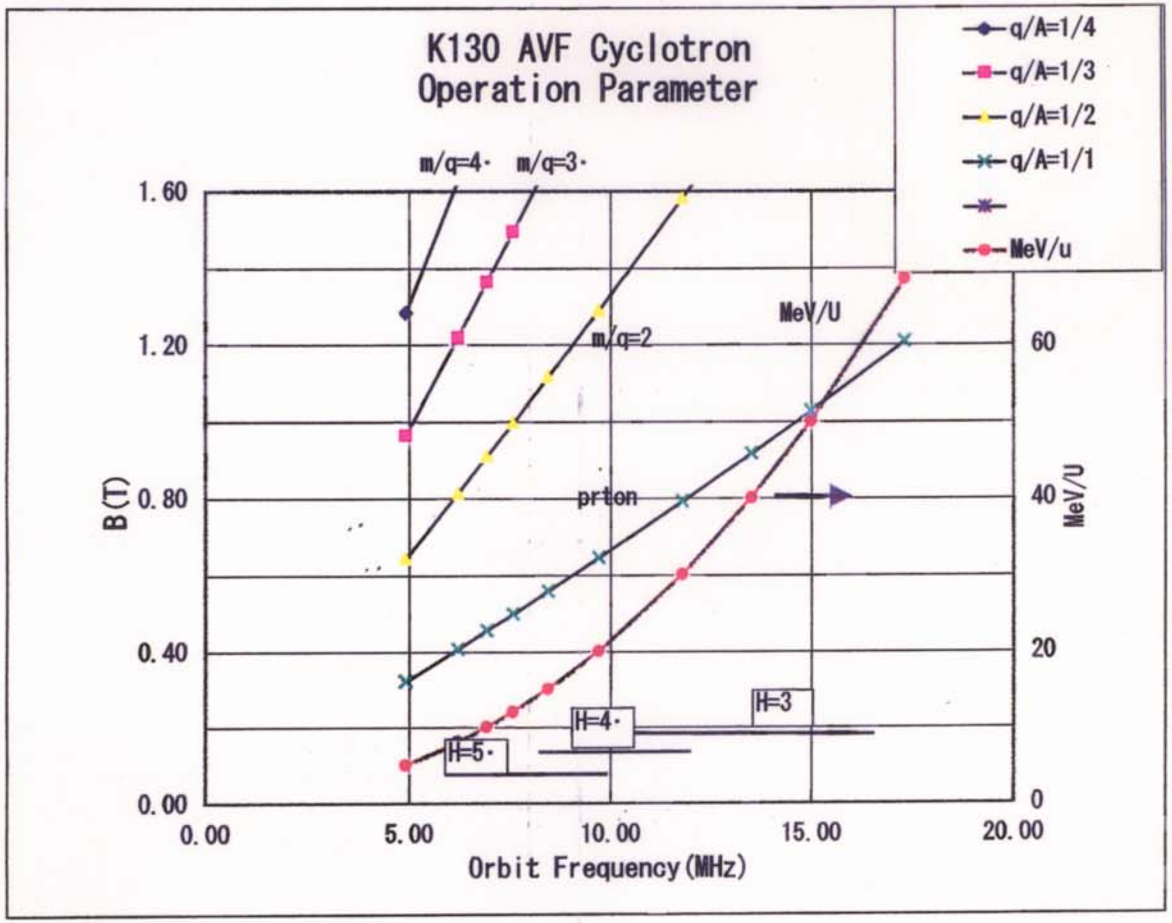

2002年3月5日

図3　磁場計算1例

（ヒルギャップ：70mm、バレーギャップ：1600mm）

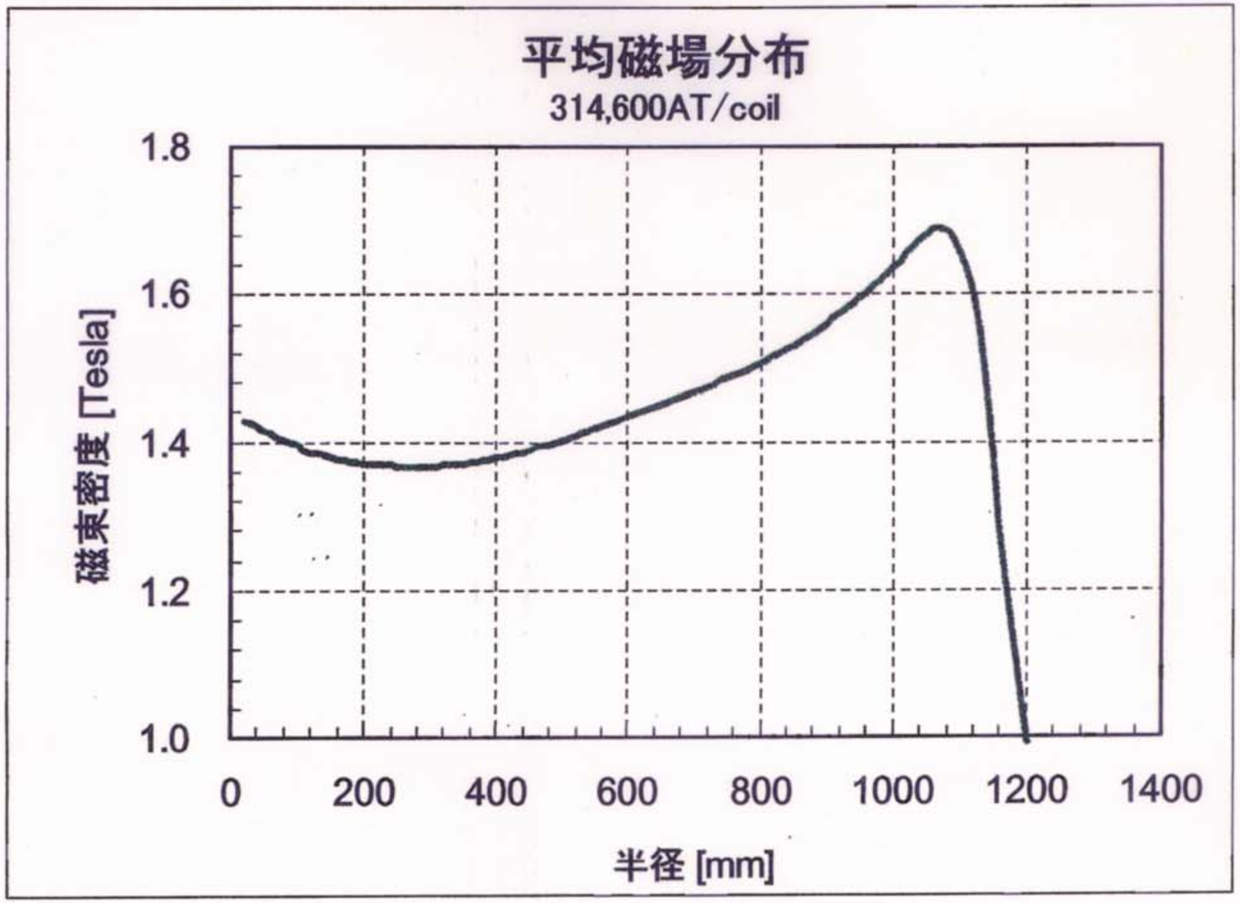

2002年3月5日

AVFサイクロの利点と問題点

利点

1. 入射エネルギーが低く、イオン源から直接入射可能。システムが簡単。
2. コイルの構造が簡単で、超伝導コイルも製作可能。
3. 小型で、安価である。

問題点

1. 空胴のスペースが狭い為、電圧があまり高く出来ない。（200kVが限界か？）
2. FT空洞を入れるスペースが狭い。
3. フラッターが小さい為、場合によってはスパイラル角をつける必要がある。

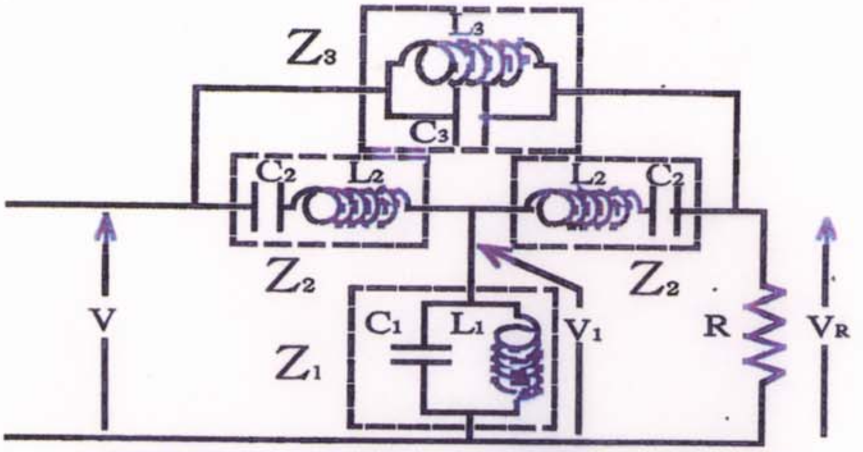

Z3
L3
C3
C2
L2
Z2
V
C1
L1
Z1
V1
R
VR

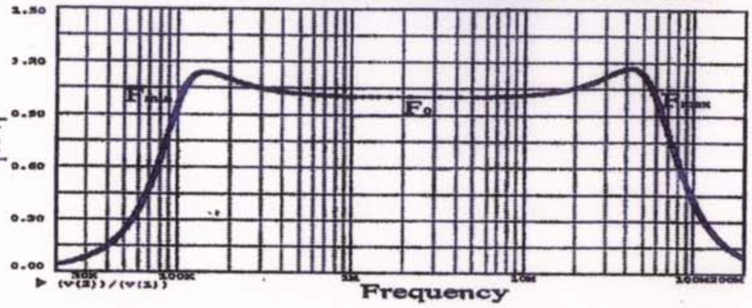

|VR/V|
F0
Frequency

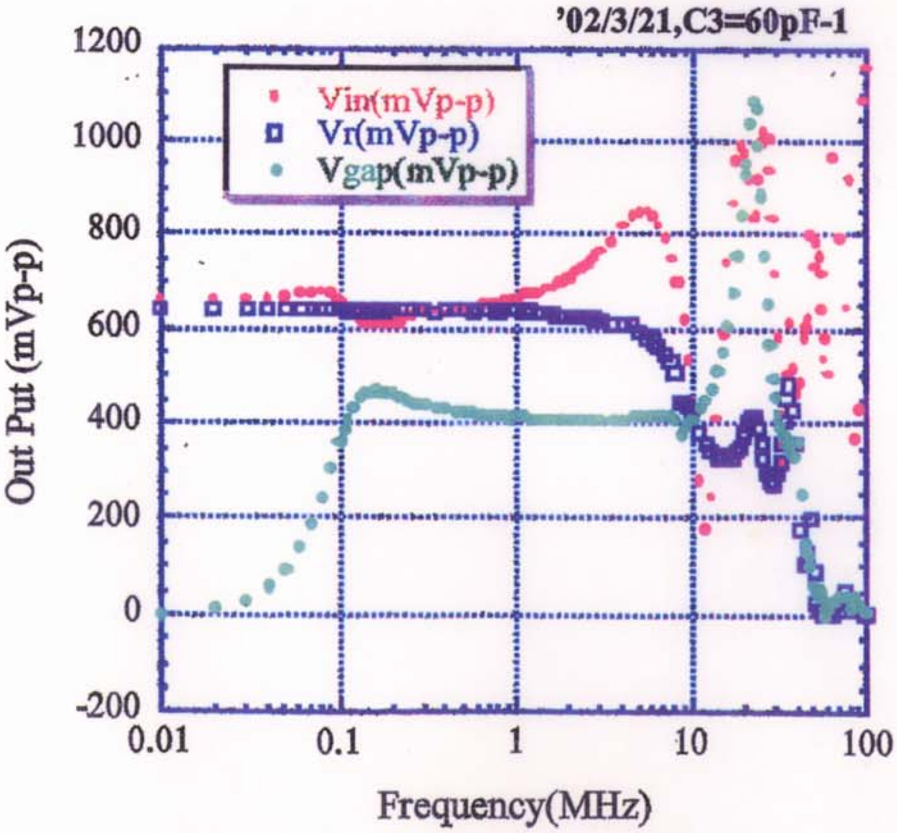

'02/3/21,C3=60pF-1
Vin(mVp-p)
Vr(mVp-p)
Vgap(mVp-p)
Out Put (mVp-p)
1200
1000
800
600
400
200
0
-200
0.01
0.1
1
10
100
Frequency(MHz)

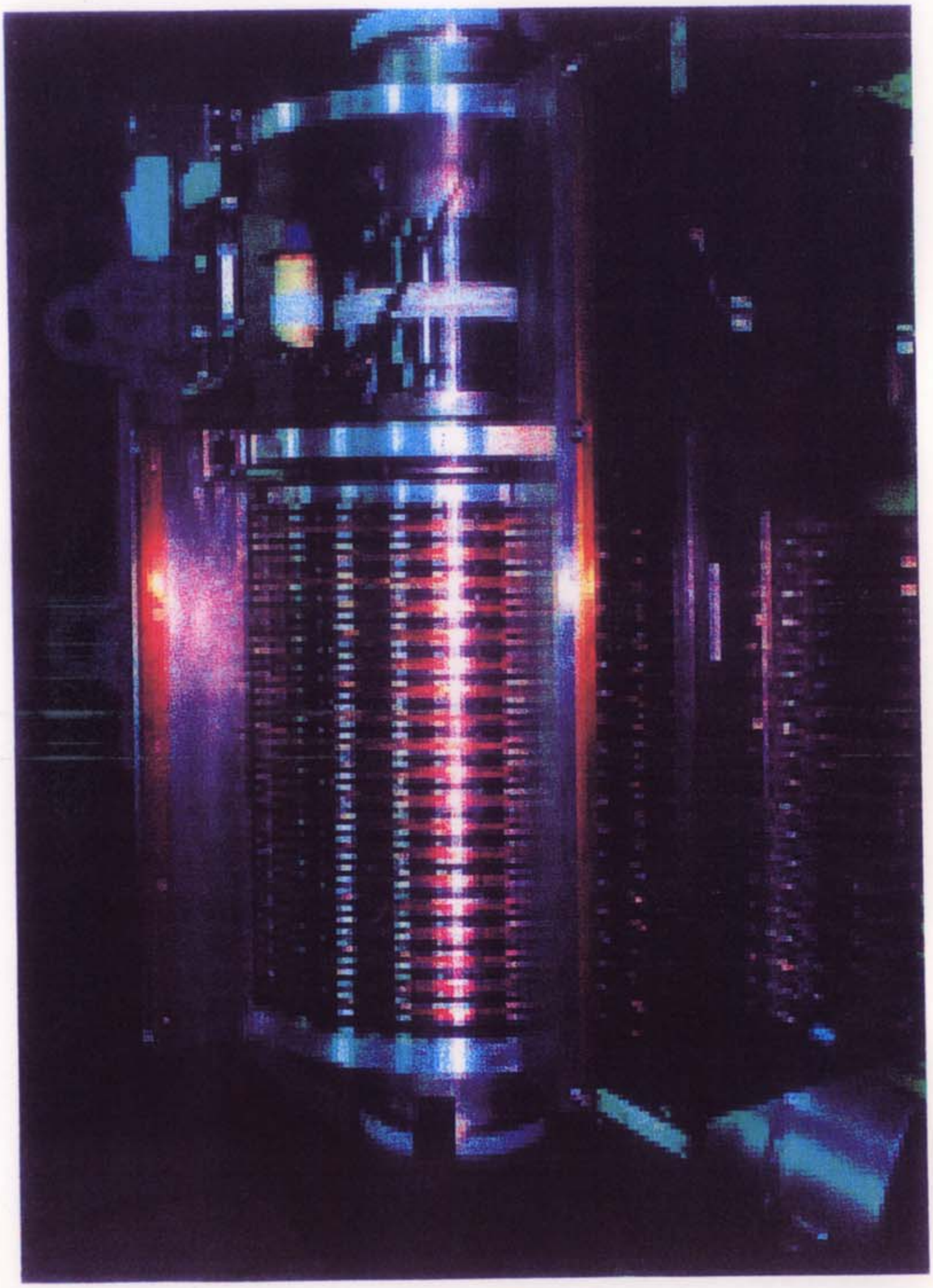

F_{max}(MHz)間で+90°〜-90°迄変化しており、0.5 M

ら+12°まで変化していると等価回路計算で求めら

い加速gap電圧波形を調べる。

まず始めに1 MHz 鋸波信号を2kw Ampで増幅し

gap電圧波形からテスト無同調Cavityの周波数帯域

鋸波入力信号とCavity加速gapに発生した波形の写

$f_{rep.}=1MHz$

$h=12$

$+\sum f_h$

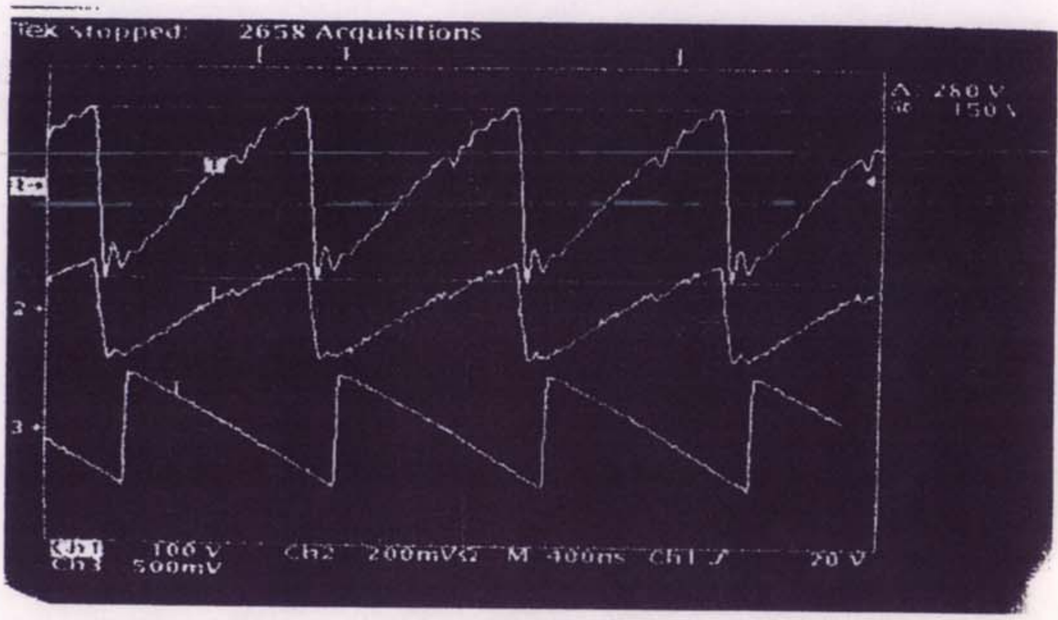

Fig.6　写真は、1.0MHz鋸波入力信号を2kw Ampで増幅した後

(上) は加速gap鋸波V_1電圧 (280 Vp-p)、(中) は加速gap電圧モ

信号源波形 AFG2020 (テクトロニクス社製) 電圧(1.0Vp-p)で

Fig.6の波形で、信号源波形と加速gap電圧波形が